

UNCLASSIFIED

AD 667 387

SUMMERTIME MARINE AIR PENETRATIONS TO THE CITY
OF SACRAMENTO

Stephen John Savage

San Jose State College
San Jose, California

August 1967

Processed for . . .

DEFENSE DOCUMENTATION CENTER
DEFENSE SUPPLY AGENCY



U. S. DEPARTMENT OF COMMERCE / NATIONAL BUREAU OF STANDARDS / INSTITUTE FOR APPLIED TECHNOLOGY

**Best
Available
Copy**

AD 667 387

SUMMERTIME MARINE AIR PENETRATIONS TO THE
CITY OF SACRAMENTO

STEPHEN JOHN SAVAGE

**SUMMERTIME MARINE AIR PENETRATIONS
TO THE CITY OF SACRAMENTO**

**A Thesis
Presented to
the Faculty of the Department of Meteorology
San Jose State College**

**In Partial Fulfillment
of the Requirements for the Degree
Master of Science**

**by
Stephen John Savage (Capt USAF)
August 1967**

APPROVED FOR THE DEPARTMENT OF METEOROLOGY

Arnold Steen

J. G. Thompson

C. A. Riegel

J. H. Wang

APPROVED FOR THE COLLEGE GRADUATE COMMITTEE

J. L. Brown

ACKNOWLEDGEMENTS

Many individuals have contributed to the writing of this paper. Probably the most important contributor was Mr. Milo Radulovich, Fire Weather Meteorologist at the Weather Bureau Office in Sacramento. It was through his suggestions that the writer first became interested in this subject. Mr. Radulovich provided much of the initial guidance during the early stages of this paper.

Certainly Mr. James Miller, Meteorologist in Charge of the Weather Bureau in Sacramento, deserves thanks for his aid and understanding in letting the writer work on this project while he was employed at the Sacramento office. Much of the data collection and tabulation was done during this time. Without the cooperation of Mr. Miller, this work could not have been accomplished.

The entire staff of the Sacramento Weather Bureau Office have been most helpful in extending suggestions and furnishing aid to the writer as well as lending him the use of needed facilities. Mr. William Thorpe of television station KCHA in Sacramento was indispensable in gaining access to wind information from the television tower at Walnut Grove, California.

The writer's thesis adviser, Mr. Jack Thompson, has provided more than the necessary amount of help in the

preparation of this paper. The writer is indebted to him especially for his aid in the use of statistical techniques in the development of the forecasting system.

Finally, the writer wishes to thank his mother and brother who, respectively, typed the initial drafts of the paper and aided in the transcribing of much of the data used in the forecast systems.

TABLE OF CONTENTS

CHAPTER	PAGE
I. INTRODUCTION	1
II. DATA COLLECTION AND SEA BREEZE THEORY	4
Observational Data	4
General Discussion of the Sea Breeze	5
III. GENERAL CLIMATOLOGY AND TOPOGRAPHY	9
Topographical Influences of the Area	9
Climate and Large Scale Influences of the Area	10
Horizontal Pressure Distribution and Flow Patterns	15
Horizontal Temperature Distribution	16
IV. MARINE AIR PENETRATION MODEL	21
Class I	22
Class II	27
Class III	31
V. THE FORECASTING TECHNIQUES	36
Statistical Methods	36
Forecasting the Marine Penetration	39
Method	39
Results	48
Forecasting the Maximum Temperature	54
Method	54

	vi
CHAPTER	PAGE
Results	55
VI. CONCLUSION	66
REFERENCES	68
APPENDIX	70

LIST OF TABLES

TABLE	PAGE
I. Average Time of Maximum Temperature from the Bay Inland	20
II. Classification System	35
III. Marine Penetration Independent Variables . . .	40
IV. Comparison of Forecast Occurrences of Y_5 to Actual Occurrences of X_7 Dependent/Independent Data	50
V. Marine Penetration Forecast Dependent Data Contingency Table	53
VII. Maximum Temperature Independent Variables . .	55
VIII. Comparison of Forecast Occurrences of Z_5 to Actual Occurrences of X_7 Dependent/Independent Data	62
IX. Maximum Temperature Forecast Dependent Data Contingency Table	64
X. Maximum Temperature Forecast Independent Data Contingency Table	65
XI. Average Pressure of Inversion Base (OAK) and Pressure Differences at 0500/1700 PDT Based on 92 Cases in 1966	71

TABLE

viii

PAGE

XII. Range of the Pressure of the Inversion Base (OAK) and Pressure Differences at 0500/1700 PDI Based on 92 Cases in 1966	72
XIII. Marine Penetration Forecast Data	73
XIV. Marine Penetration Forecast Check Data	80
XV. Maximum Temperature Forecast Data	82
XVI. Maximum Temperature Forecast Check Data	90

LIST OF FIGURES

FIGURE	PAGE
1. Station Locations and Topography of the Data Area	6
2. Topographical Cross Section through the Coastal Mountains	10
3. Summertime Pressure Patterns of the West Coast.	14
4. Normal Flow Patterns Found in the Marine Layer During Summer	16
5. Average Maximum Temperature Isotherms for July.	19
6. Pacific High Pressure Cell Displaced Seaward .	23
7. Maximum Temperature Isotherms for Class I Day of July 6, 1966	26
8. Pacific High Pressure Cell Displaced Inland . .	32
9. Marine Penetration Forecast Graphs	43
10. Maximum Temperature Forecast Graphs	56

CHAPTER I

INTRODUCTION

Summertime weather forecasting in the Sacramento Valley is usually a fairly routine procedure. Normally, the sky is clear, the temperature high, and the humidity low. However, the penetration, from the San Francisco Bay region, of cool, moist marine air into the Sacramento Valley area is an exception to the normal weather. Such intrusions can cause the maximum temperature to fall 25°F or more and the relative humidity to increase by 30 per cent in 24 hours. In addition, the intrusion is accompanied by strong, gusty winds in its initial stages.

One important reason for being concerned with marine intrusion is that it has an effect on forest and grass fires. When high daytime temperature and low relative humidity persists for any great length of time, the danger of fire in the Valley and surrounding foothills becomes extreme. The low temperature and high humidity of marine air alleviate the fire danger. However, if an intrusion of marine air occurs after a fire has started, high winds during the early stages of the intrusion fan the flames and can drive the fire out of control. The high winds generally subside after the initial intrusion and then the marine air

is an asset to fire control. The meteorological conditions associated with the onset, persistence, or absence of marine air in the Valley are, therefore, of paramount importance to those concerned with fire control.

Sports activities at Folsom Lake are also affected by the marine intrusion. Strong winds during the incursion of the marine air make swimming and boating hazardous. Suitable warnings to the public could be made if such intrusions could be accurately forecasted.

Many other agencies in the Sacramento area are affected by the high winds usually associated with the incursion of marine air. Generally, wind speeds in excess of 20 miles per hour are considered significant enough to warrant taking protective measures. Commercial and public organizations such as Aerojet General, Douglas Aircraft, and the Port of Sacramento, need to know in advance when they should implement protective measures against such winds. It has not, however, been possible to objectively forecast the occurrence of a marine intrusion. The purpose of this study is to provide a means for making such forecasts.

Several studies have been conducted on the nature of marine penetrations into coastal valleys. These include investigations by Lowry (1959), Fosberg and Shroeder (1966),

and Schultz (1961) dealing with descriptions of the phenomenon and its effects upon agriculture and forestry. In addition, several attempts have been made to forecast maximum temperatures in Sacramento: Harwan (1960) and Sinclair (1961) both dealt with this problem; however, their forecast systems dealt only partially with the marine penetration factor. No one, to the investigator's knowledge, has conducted a detailed examination of the physical aspects of the marine penetration into the Sacramento area and coupled it with a forecast system.

The overall goals of this study are (1) to describe the physical characteristics of the marine intrusion, (2) to establish a simple model describing its operation, and (3) to develop (a) a scheme for forecasting marine intrusions and (b) an objective technique for predicting the maximum temperature at Sacramento.

CHAPTER II

DATA COLLECTION AND SEA BREEZE THEORY

Observational Data

The summer of 1966 was the time of most active data collection. Most of the physical description was gleaned from these data. Data from 1965 and 1966 were used to develop the forecast techniques, while random selections from the summers of 1958 and 1964 were used as independent data to check the techniques.

Since the major aim of this study was to develop forecast techniques to be used on a routine basis, only currently available weather observations were used. No special instrumentation was used, with one exception. A 1,500-foot television transmission tower located at Walnut Grove, California, lies along the path that marine air must follow to reach Sacramento. Wind speeds, measured with cup anemometers located at the 450- and 1,500-foot levels of the tower, were received at 0530 and 1530 hours PDT daily. Unfortunately, wind directions were not available.

With the exception of that obtained from the television tower, all other data for this study came from standard Weather Bureau sources. Observational data

5

included temperature, pressure, wind speed and direction, dew point, cloud cover, and upper air data from both pilot balloon (PIBAL) and radiosonde observations (RAOB) taken at Oakland, California (RAOB and PIBAL); Red Bluff and Fresno, California (PIBAL only); and Reno, Nevada (PIBAL only).

First order and supplementary airways stations of the United States Weather Bureau were used for standard meteorological data, while cooperating observer stations were used for maximum temperature readings. The network of stations used is shown in Figure 1.

General Discussion of the Sea Breeze

The sea breeze circulation occurs along many coasts of the world. Because of the different heating characteristics of land and water, air over the land becomes much warmer during the day than that over a water surface. Upward movement of the overland air due to buoyant forces upon it produces a pressure gradient aloft directed from land to sea resulting in upper-level seaward movement of the air. According to Riehl (1954), in response to this mass divergence of air in the upper levels, low-level pressures begin to fall establishing a low-level pressure gradient from sea to land. Cooler, more dense, marine air responds to this gradient by moving onshore, and the sea

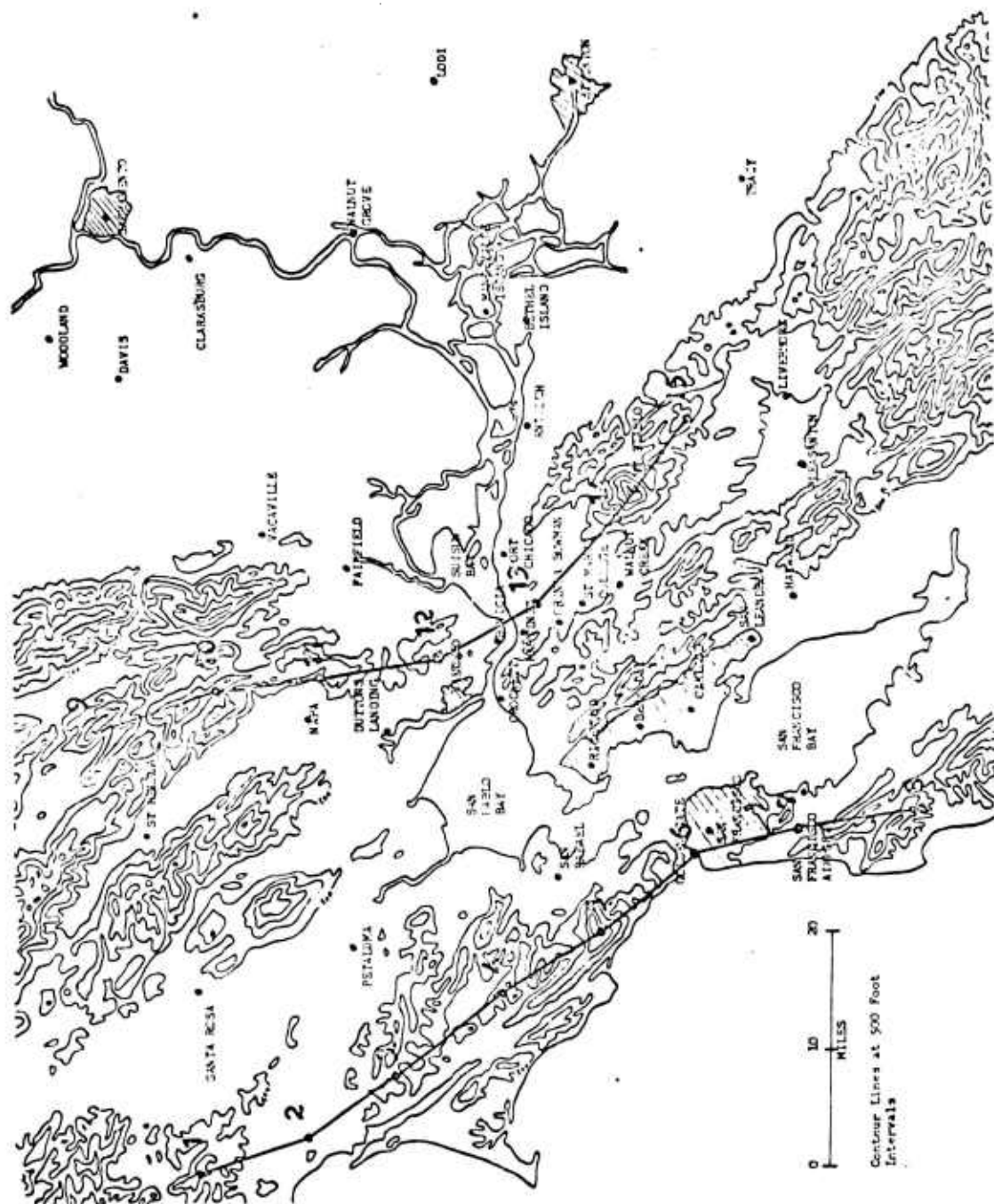


Figure 1. Station locations and the vicinity of the study area.
See Figure 2 for significance of numbered points.

breeze circulation is established.

According to Wallington (1961), the distance inland to which the sea breeze is able to penetrate is dependent upon a number of factors. First, the strength of the solar radiation: increased insolation tends to increase the land-sea temperature gradient. Second, the direction and strength of any superimposed general wind flow: large scale winds in the same direction as the sea breeze will tend to reinforce the sea breeze flow. Third, the depth of the marine layer: a deeper layer is capable of greater inland penetration in unmodified form than a shallow one. Fourth, the sea temperature: cooler water offshore increases the land-sea temperature gradient.

As the land-sea temperature contrast increases, the pressure gradient between land and sea increases, and the sea breeze accelerates. According to Haurwitz (1947) and Schmidt (1947), with no retarding forces, the sea breeze will continue to accelerate for as long as a land-sea temperature gradient exists. This will yield a maximum sea breeze speed well after the maximum temperature difference between land and sea occurs. However, because a certain minimum temperature difference is required to overcome the effect of friction, the sea breeze usually attains its maximum speed at, or shortly after, the maximum

temperature difference is observed.

Another influence is the Coriolis acceleration, which, over a period of time, deflects the sea breeze from a direction perpendicular to the coast to one which is more parallel to the coast. The sea breeze is, in a sense, self-regulatory. As the sea breeze becomes stronger, more marine air is advected inland. This reduces the difference in temperature and density between the land and sea air. As the contrast is reduced, so is the pressure gradient, and the sea breeze gradually begins to lose strength, eventually dying out altogether.

CHAPTER III

GENERAL CLIMATOLOGY AND TOPOGRAPHY

Topographical Influences of the Area

The onshore pressure gradient produced by differential land-sea heating causes a sea breeze to occur along practically the entire California coast. However, except for certain low-lying gaps in the mountains where marine air can flow inland, the Coastal Mountains effectively block marine penetrations into the Central Valley (Figures 1 and 2).¹ The principal gaps include:

1. Petaluma Gap - Northwest of San Francisco. Elevations less than 500 feet.

2. San Bruno Gap - Just south of San Francisco. Elevations about 200 feet.

3. Golden Gate - Sea level passage into San Francisco Bay.

4. Carquinez Strait - Northeast of San Francisco connecting San Pablo Bay to Suisun Bay. Provides sea level passage into Central Valley.

The city of Sacramento is located in the northern half of the broad Central Valley of California. The Coastal Mountain Range, with average elevations of 2,500

¹The numbered points connected by lines in Figure 1, page 6 show the path followed in constructing the cross section shown in Figure 2. The numbers along the base of the cross section in Figure 2 correspond to the numbered points in Figure 1.

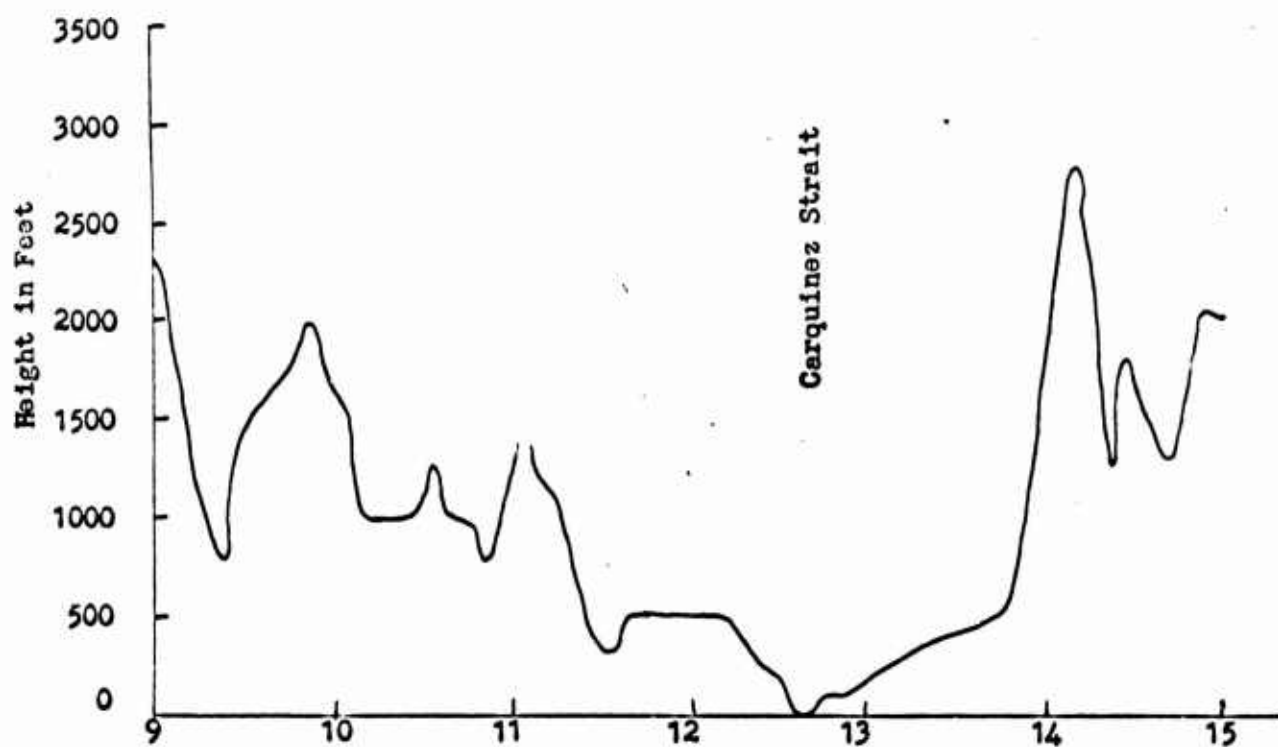
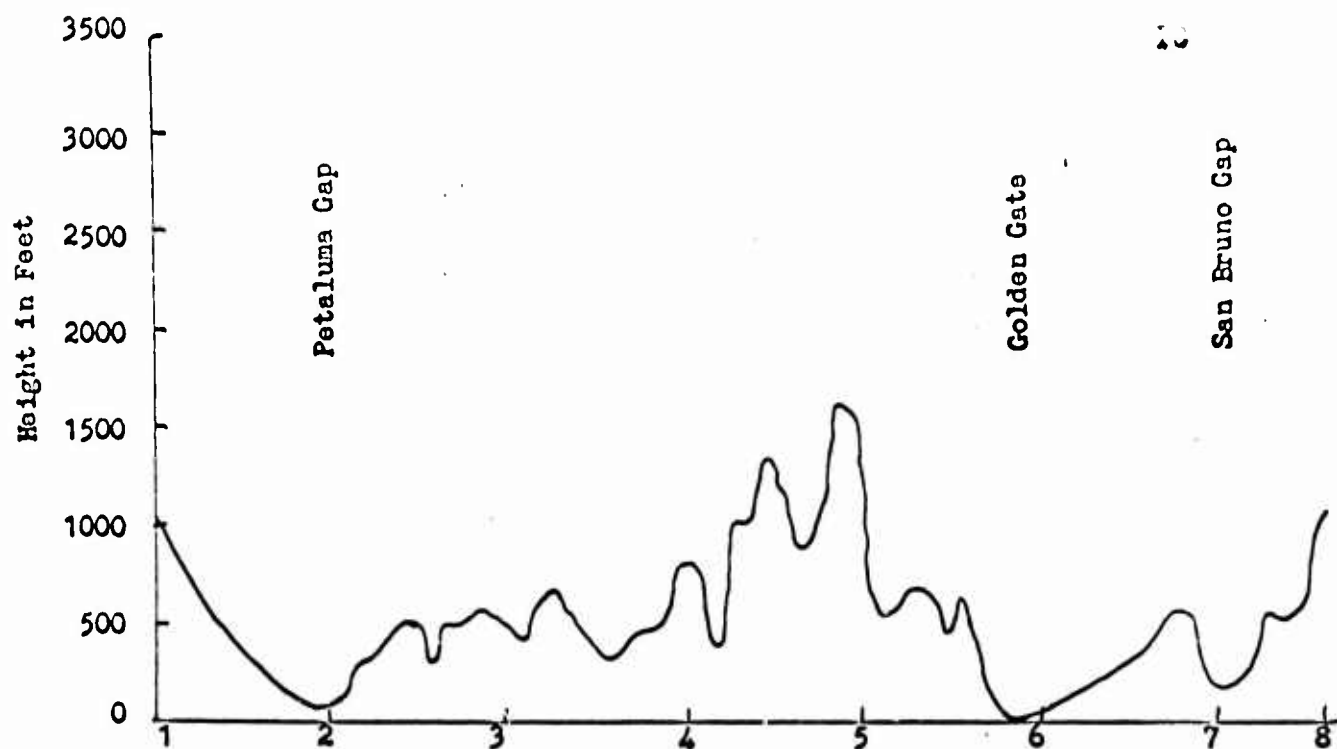


Figure 2. Topographical cross section through the Coastal Mountains. Numbers correspond to numbered points in Figure 1.

feet, lies 40 miles to the west of Sacramento, while the Siskiyou Mountains lie 160 miles to the north and the Sierra Nevada Mountains are 30 miles to the east. Southward, the Valley extends, uninterrupted, for 280 miles ending against the Tenachapi Mountains. The Valley floor is essentially flat, with elevations seldom above 200 feet.

Off the coast, the ocean bottom drops rapidly. The California Current, driven by the steady northwesterly flow around the eastern edge of the Pacific high, flows southward along the California coast. Coriolis effects acting on the current impart a general offshore movement to the surface water inducing a pronounced upwelling of deep, cold water off the coast. The upwelling produces a band of cold water approximately 80 miles wide off San Francisco (Williams, 1968). Surface water temperatures during July are only about 54°F.

The primary source of marine air is the Pacific Ocean. Marine air entering the San Francisco Bay or Central Valley must, in general, pass through the Golden Gate or over the northern end of the San Francisco Peninsula and turn northeastward to reach the Carquinez Strait. The Petaluma Gap appears to be less favorable for marine intrusions and contributes very little to marine air in either the San Francisco Bay or Central Valley.

As the marine air moves inland, it is modified by the surface over which it passes, the modification depending, in large part, on the temperature of the underlying surface. The San Francisco-San Pablo Bays, however, play an important role in preventing extensive modification of the marine air as it moves inland. The temperature of the waters of these two Bays is cooler than the surrounding land area during the summer. Hence, air passing over them will not be modified to any great extent.

Williams (1966) states that the Bays themselves are kept cool by the tidal exchange of water with the Pacific Ocean through the Golden Gate. Similarly, the temperature of Suisun Bay water is kept low through exchange with waters of the San Francisco and San Pablo Bays, via the Carquinez Strait. Tidal currents through these restricted channels can reach six knots or more.

Tidal flushing is less effective in keeping water temperatures low in the large areas of shallow water (less than 10 feet) than in the deeper areas of the Bays. Even in these areas, however, the temperature of the water does not exceed oceanic water by more than 15°F . Thus, oceanic air moving over the Bays appears to be only slightly modified before it reaches the land.

Climate and Large Scale Influences of the Area

In the summer months, the air temperature increases from the Bay area, through the Carquinez Strait, and northward up the Valley to the Siskiyou Mountains. The semi-permanent Pacific high pressure cell reaches its maximum development at this time and dominates the area (Figure 3). Cyclones rarely reach the California coast. Meteorological conditions existing along the coast are characterized by northwest winds, subsidence, and scant precipitation (Byers, 1931).

Generally, a "heat trough" can be found extending up the Central Valley from the Sonoran-Mojave Desert (Figure 3). The general pressure gradient is, therefore, onshore. A temperature inversion, associated with subsidence in the Pacific high, is usually located over the area. Cooling of the marine air at its base by contact with the cold water offshore and subsidence-induced warming aloft combine to strengthen the inversion.

Air approaching the California coast will be cool and moisture laden due to its long overwater trajectory. As it flows across the cold band of water offshore, it is further cooled, accentuating the temperature contrast between land and water. The cooling is often sufficient to cause some of the moisture to condense producing the high incidence of fog and stratus along the California

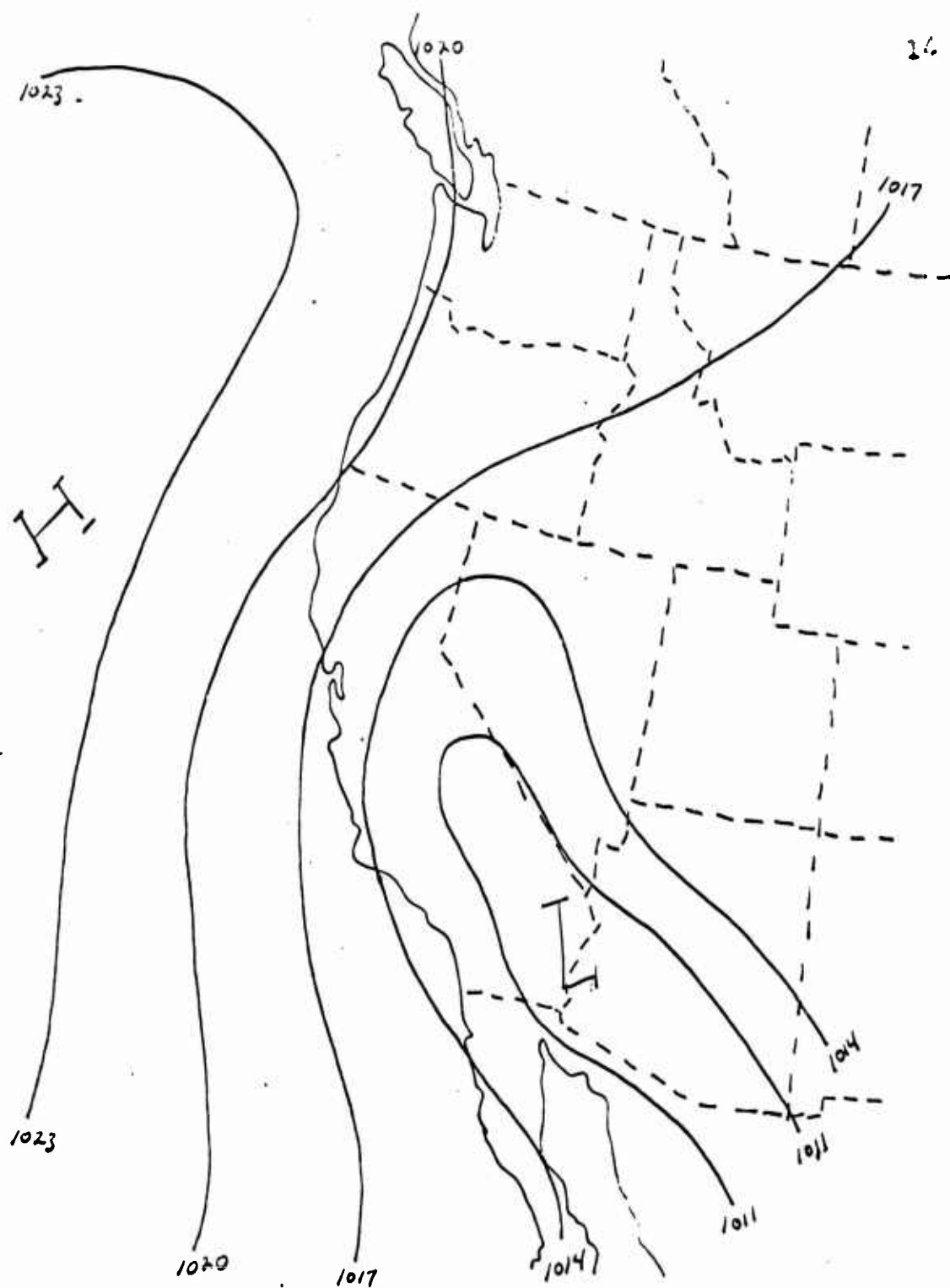


Figure 3. Summertime pressure patterns of the west coast (Williams 1966).

coast in the summer (Patton, 1936).

Horizontal Pressure Distribution and Flow Patterns

The normal pressure distribution for July (Figure 3) shows the Pacific high pressure cell located well off the coast and a thermal trough located inland over the Central Valley (Neiburger, 1961). Higher pressures are found to the north, east, and west. These pressures are, in general, in equilibrium; however, marine air over the Bay, being colder and heavier, responds to this low pressure by flowing into the Valley.

The onshore pressure gradient and channeling effect of the coastal mountains produces the normal flow patterns to be found within the marine layer of air (Figure 4). The northwest winds found along the coast become more westerly as they are drawn into the interior through the Golden Gate and over the San Francisco Peninsula. The channeling influence of the Golden Gate produces a jet that moves eastward but tends to fan out as it moves downstream. Air peels off from this widening fan and turns southward into the Santa Clara Valley and northward into San Pablo Bay and on into the Petaluma Valley. The northward flowing current branches eastward over San Pablo Bay and flows through the Carquinez Strait into the Central Valley. The Strait also channels the flow into a jet which fans out, turning northward and southward in the Sacramento Valley.

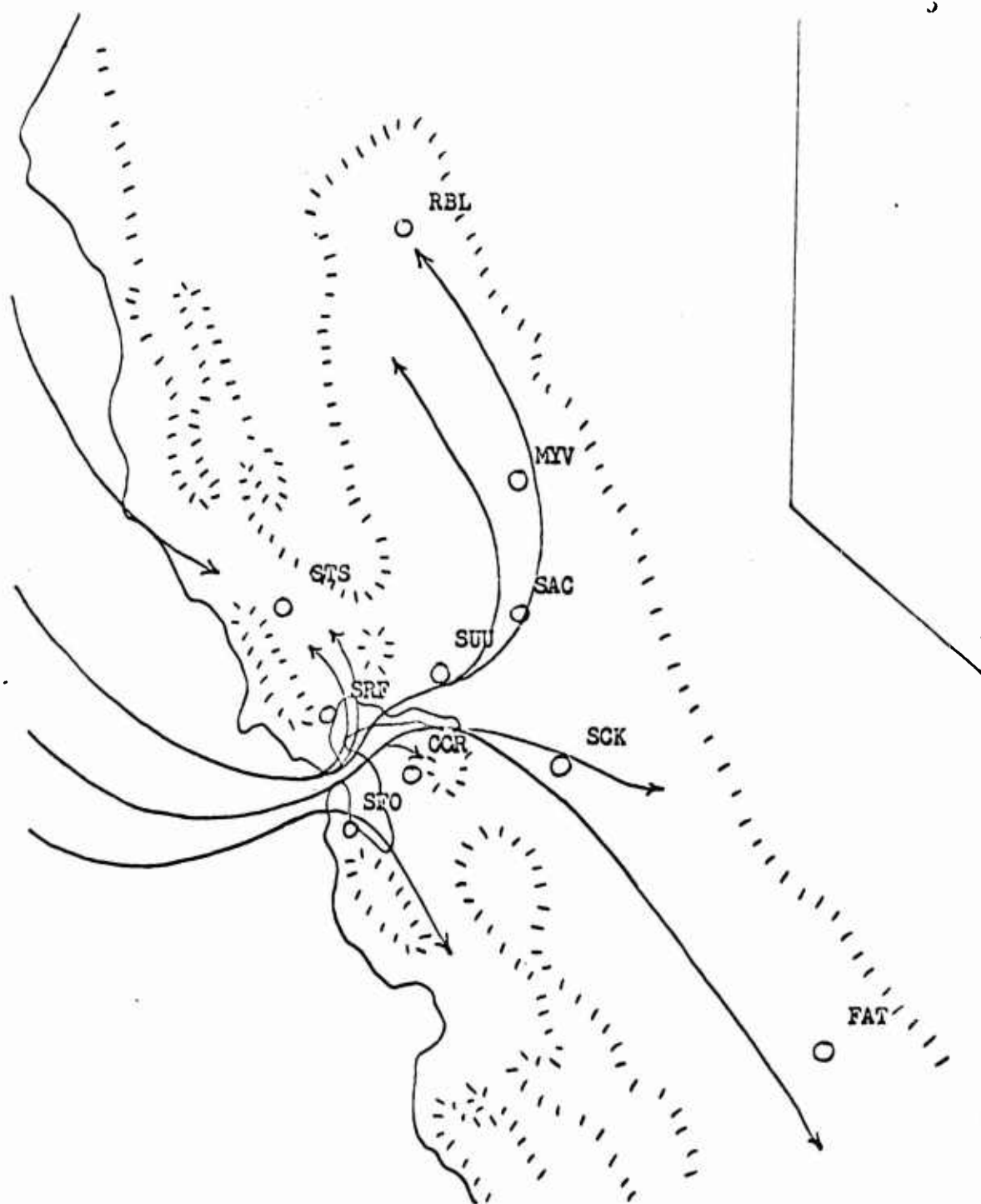


Figure 4. Normal flow patterns found in the marine layer during summer (Root 1960).

As a result, the winds observed at Sacramento in summer are usually from the southwest.

The sea breeze along the coast begins late in the morning or early afternoon. At first, even low lying obstructions may act to block the sea breeze so that only the Golden Gate serves as a passage inland for it. As the day progresses, the sea breeze layer deepens (see Edinger 1959, Raupen 1969, and Williams 1966), due to turbulent mixing induced by surface heating and wind mixing induced by the increasing speed of the sea breeze flow, and begins to flow over the low lying hills of the San Francisco Peninsula. The breeze may develop from the Bay also and begin to move eastward. The two flows, oceanic and bay, eventually merge and flow through the Carquinez Strait arriving in Sacramento late in the afternoon or early in the evening, as a strengthening of the southwesterly winds.² The depth and intensity of the marine layer determines, in large part, whether the breeze will reach Sacramento and how intense it will be. The marine layer depth, in turn, is controlled by the height of the subsidence inversion associated with the Pacific high. When the high is displaced onshore, the subsidence effect is greatest and the inversion reaches its maximum intensity. At this time, the

²At times, the sea breeze may develop solely from the Bay and there will be no combination of oceanic and bay flows.

10

marine layer is very shallow (indeed it may be entirely eliminated). If it is present, it will be quickly modified as it moves onshore over the warmer land. The influence of the sea breeze will be felt for only a short distance inland. In addition, the shallow nature of the marine layer prevents it from flowing over the higher elevations of the coastal hills which extend north and south of the Carquinez Strait.

Occasionally, the Pacific high may be displaced far offshore and, under the influence of decreasing subsidence, the marine layer will reach depths sufficient for it to move inland with very little modification. The coastal hills provide very little blocking effect under these conditions, and the marine air may extend deep into the Central Valley.

Horizontal Temperature Distribution

During the summer, the temperature difference between ocean water and land surfaces may become as much as 35°F or more in the afternoon. A chart of mean maximum temperatures for the month of July (Figure 5) shows the strong afternoon temperature gradients which develop along the edges of the various water surfaces and the tongues of cool air that extend across the San Francisco Peninsula, southward into the Santa Clara Valley, northward into the



Petaluma Valley, and eastward through the Carquinez Strait. The bulge in the isotherms through the Strait is representative of marine incursions through the Carquinez Strait on the average. (June and August isotherm patterns are similar to July's, but with slightly lower temperatures.)

It should be realized that the chart does not represent the temperature distribution at the same instant because the maximum daily temperature is not reached at the same time at all locations. Due to the cooling influence of the sea breeze, the daily maximum is usually reached earlier in the day at locations near the Bay than at those in the Central Valley. See Table 1.

TABLE 1
AVERAGE TIME OF MAXIMUM TEMPERATURE
FROM THE BAY INLAND*

<u>City</u>	<u>Time of Maximum Temperature</u>
San Francisco	1430 PDT
Oakland	1530 PDT
Fairfield	1603 PDT
Sacramento	1646 PDT

*Based on 92 cases from June, July, and August 1966. Times were estimated from hourly observations of the U. S. Weather Bureau.

CHAPTER IV

MARINE AIR PENETRATION MODEL

The forecast system developed in this study was constructed from a "marine penetration model" which describes the nature of the pressure distribution, and the resulting wind and temperature patterns which are believed to be related to the advection of marine air into the Sacramento--and to some extent the San Joaquin--Valley of California. The model involves the delineation of three classes of weather patterns, each class being related to the subsequent presence or absence of marine air in the Valley and to the corresponding temperature, pressure, and flow characteristics typical of the class.

In the chapter, an attempt will be made to analyze the various summertime weather patterns, placing them in one of the three classes. Once this has been accomplished, it will be possible to describe, label, and forecast the classes using an appropriate statistical technique. The statistical application of the model to the forecast system will be discussed in the next chapter. In describing each class in the model, the synoptic situation and meteorological conditions which occur during the existence of that class will be discussed.

Class I

Class I days are associated with a general penetration of marine air into the Sacramento Valley. The flow of cool marine air causes maximum temperatures to be below the seasonal normal in Sacramento.¹ During the Class I period, the eastern portion of the Pacific high reaches its maximum seaward displacement, while inland, a general area of low pressure exists over Oregon and Nevada (Figure 6).

With the high pressure cell located offshore, subsidence associated with the eastern portion of the high is at a minimum and the marine layer reaches its maximum depth. Marine air flows through the Carquinez Strait and over all but the highest of the coastal mountains in a broad, deep layer that is modified only slightly by the underlying land. At times, coastal stratus may be advected into the Sacramento River Delta area reducing solar insolation so that neither the land beneath nor the marine air above is heated, further reducing modification of the air.

The low pressure area located to the north and east results in a northward directed pressure gradient in the Valley, while high pressure over the ocean to the west causes a well developed onshore gradient. The result is a

¹The seasonal normal ranges from 81°F in early June to a high of 91°F in mid-July.

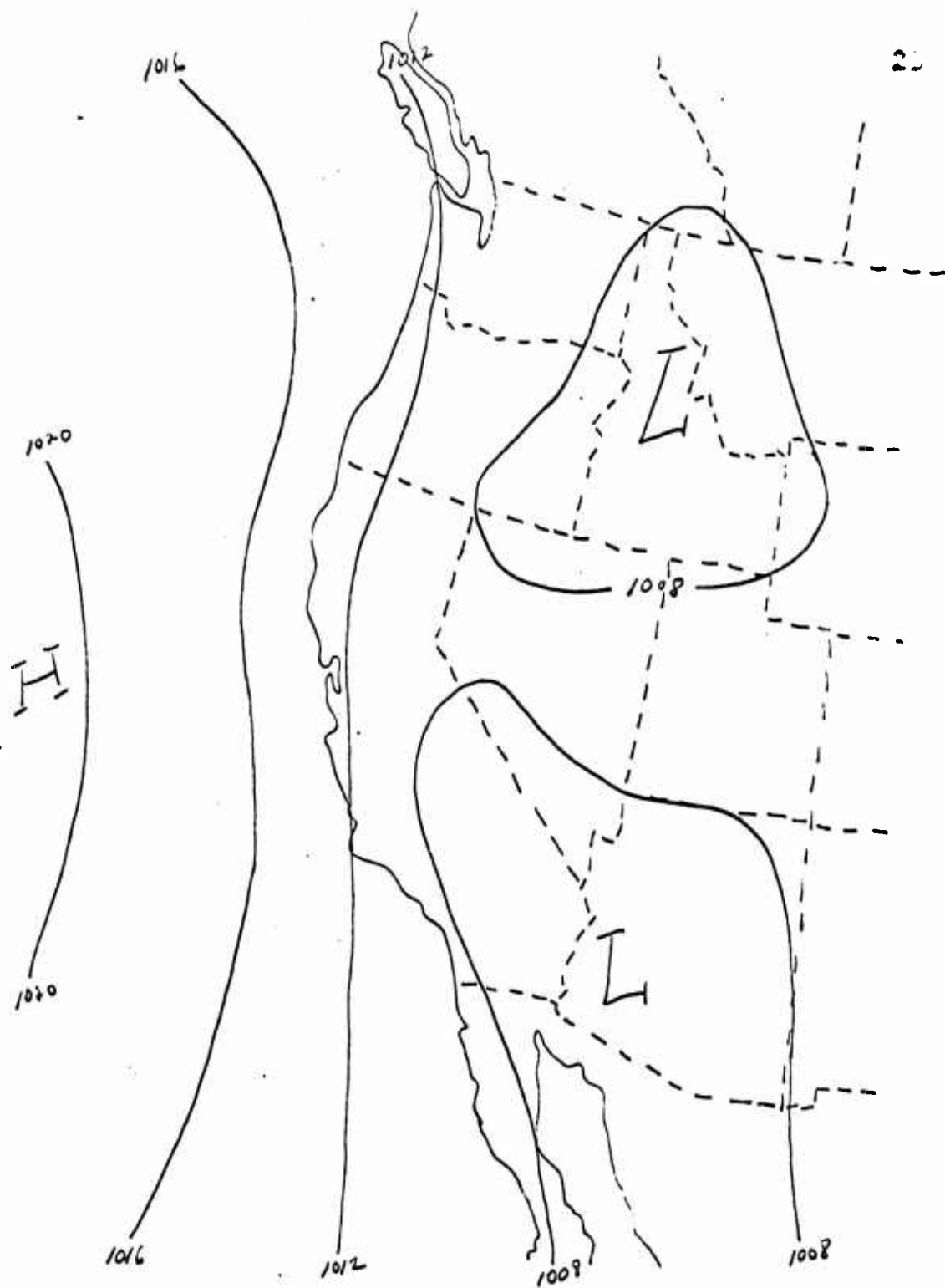


Figure 6. Pacific high pressure cell displaced seaward.
(composite from NMC analysis of Class I
weather map).

strong (over 11 knots), gusty southwesterly wind in Sacramento. Unlike the winds normally associated with a sea breeze circulation which arise due to surface heating (in the afternoon) and end with cessation of that heating (at sunset), the marine penetration begins at any time when the synoptic situation is favorable and may continue throughout day or night. The intensity of the penetration is, in large part, dependent upon the depth of the marine layer and intensity of the south to north pressure gradient.

Aloft, a deep trough of low pressure overlies the area. The flow is well organized and quite strong from the southwest below 10,000 feet. The southwesterly flow on the east side of the trough may reinforce the surface winds on the initial day of the penetration.

The marine penetration may be a brief, one day, occurrence or it may continue for several days. Usually, the initial penetration, accompanied by strong, gusty winds, will fill the Valley with marine air. On succeeding days, the temperature will remain below the seasonal normal but the winds will be much lighter from the southwest or, quite often, from the north (from 290° - 350°). While it might be expected that north winds would prevent marine air from entering the Valley through the Carquinez Strait and, therefore, with the absence of marine air, result in warming, this is not the case. The flow is the result of the absence

of the subsidence inversion, which, with the retreat of the Pacific high has been destroyed, allows northerly flow on the west side of the trough to reach the surface. The winds advect cold air southward from northern latitudes, and do not result in warming but instead cause cooling in the Valley. Hence, the lowest maximum temperature may be found, not on the day of the initial penetration, but on the day after.²

An interesting feature may be found in the maximum temperature isotherm patterns of Class I (Figure 7). The jet-like penetration of cold air through the Carquinez Strait thrusts deep into the Valley before fanning out to north and south. The result is a large pool of warm air on the lee side of the mountains to the north and occasionally to the south of the Strait. The marine air actually appears to enter Sacramento from the southeast rather than the southwest. The "lee side effect" causes marine air to be delayed by one day in reaching Woodland, Davis, Vacaville, and sometimes Clarksburg. Likewise, the marine air is usually one day late in leaving these areas at the end of the penetration. The pattern shown in Figure 7 is common to almost all Class I days.

²North winds may also be associated with maximum temperatures that are above the seasonal normal, as discussed in a later section.

Table II, at the end of this chapter, gives a complete breakdown of the criteria for the various classes. Class I, including the Class I associated north winds, is designated by a "1" in the forecasting system (see column headed X_7 in Table II and see the footnote at the bottom of Table II for a definition of X_7). Tables XIA and B, located in the appendix, present the vertical structure and pressure data upon which the discussion in this chapter is based. Tables XIIA and B, also in the appendix, present the variance of the data shown in Tables XIA and B.

Class II

Class II may be described as the true sea breeze or the sea breeze shear line situation. Maximum daily temperatures are equal to or greater than the seasonal normal in Sacramento during the sea breeze period. As the sea breeze begins early in the afternoon, temperatures begin to fall. With the onset of darkness, the sea breeze dissipates. The class may be divided into three groups, two of which are quite similar in effect but somewhat different in their cause.

All groups represent a slight shoreward displacement of the Pacific high with a corresponding increase in subsidence and lowering of the subsidence inversion. The resulting decrease in depth of the marine layer allows less

marine air to penetrate inland resulting in an increased rate of modification. As the marine layer depth decreases, it descends below the higher mountains to the north and south of the Carquinez Strait, so that not only a shallower but also a less extensive marine layer moves into the Valley. Nevertheless, the marine layer is still deep enough to reach Sacramento late in the afternoon as a strengthening of the prevailing southwesterly winds. If north winds are occurring in the Valley, they will be replaced by southwesterly flow.

The shoreward displacement of the Pacific high establishes a weak ridge over Washington, while the interior Valley is dominated by maximum development of the thermal trough. Pressures are higher to the north and east (as opposed to the low pressures of Class I) so that the general gradient is directed Valleyward. In the meantime, development of a deep thermal trough in the Valley coupled with the onshore location of the high pressure cell increases the onshore gradient. Pressures in the north end of the Valley fall rapidly under the intense heating, creating a northward directed interior Valley gradient by early afternoon. The marine air responds to this situation by moving into the Valley.

The Class IIA day is the true sea breeze case. In the forecast system it will be designated by a "2" (see X₇ in Table II). Responding to the intense heating of the

interior Valley, marine air moves through the Carquinez Strait and flows northward, arriving in Sacramento between 1400 and 1600 hours PDT as an abrupt increase to 11 knots or more, with stronger gusts, in the southwesterly wind (from 210° - 250°). The temperature begins a rapid decline. As sunset approaches, the winds decrease to less than 10 knots and cooling destroys the sea breeze mechanism. Because the breeze arrives so late, only minor reductions in the maximum temperature occur and temperatures still reach normal or above. Class IIA is the rarest of all weather types to occur in Sacramento.

The description of Class IIB is much the same as Class IIA. However, due to a shallower marine layer, lesser onshore gradient, and higher pressures to the north and east, the sea breeze arrives in Sacramento in highly modified form. There is only a slight increase in the southwesterly winds to greater than 10 knots, with no gusts and temperatures only slightly affected if at all.³ (This is usually manifest as a brief delay in heating until the sea breeze passes through.) The sea breeze usually begins later in the afternoon than does the Class IIA wind and is usually of only one or two hours duration. The flow is no

³The Class IIB wind usually reaches a speed of only 12 or 13 knots.

20

longer a sea breeze at all and may better be termed a "sea breeze shear line," as it represents all that remains of a highly modified sea breeze. Because of its minimal effect on Sacramento's heating and winds, the overall pattern is much like that of Class IIIA (see next section); therefore, Class IIB is grouped with Class III in the forecast system and is designated by a "3". The Class IIB day is the most frequently occurring weather type in Sacramento during the summer.

The physical description of Class IIC is much like that of Class IIA; that is, an afternoon increase of the southwesterly winds to 11 knots or more, with gusts, and a rapid decrease in temperature. However, instead of decreasing at sunset, the wind usually continues blowing at greater than 10 knots throughout the night and develops into a full marine penetration (Class I) by early morning. For this reason, the Class IIC sea breeze has been labeled the pre-marine penetration sea breeze. It is the result not only of interior Valley heating and weakening of the surface high pressure ridge but also of a general retreat of that ridge with the attendant development of low pressures to the north and east. The lowering pressures allow a continued northward directed gradient after the sun has set; hence, the continued flow of marine air into the Valley. For classification purposes, Class IIC will be designated by a

"2" in the forecasting system.

Aloft, a weak ridge or a short wave trough may be found in association with Class IIA and IIB; however, Class IIC is associated with the onset of an upper level low pressure trough which deepens and leads to Class I. Winds aloft below 10,000 feet are well developed from the southwest and usually quite strong for both Class IIA and IIC, while for Class IIB, the winds are light and variable. Television tower winds are generally light in the morning, but may be somewhat stronger in the afternoon for all three classes. Occasionally, a Class IIC sea breeze may occur after a marine penetration instead of before.

Class III

Class III defines those situations when there is either no marine air in the Valley, or the marine layer is so shallow that solar heating modifies it before it reaches Sacramento. In either case, daytime maximum temperatures in Sacramento are above the seasonal normal.

Class III may be divided into two groups, Class IIIA, which represents daylong southwesterly flow of less than or equal to 10 knots at Sacramento, and Class IIIB, which represents daylong northerly flow. Both groups represent a shoreward displacement of the eastern portion of the semi-permanent Pacific high pressure cell (Figure 8),

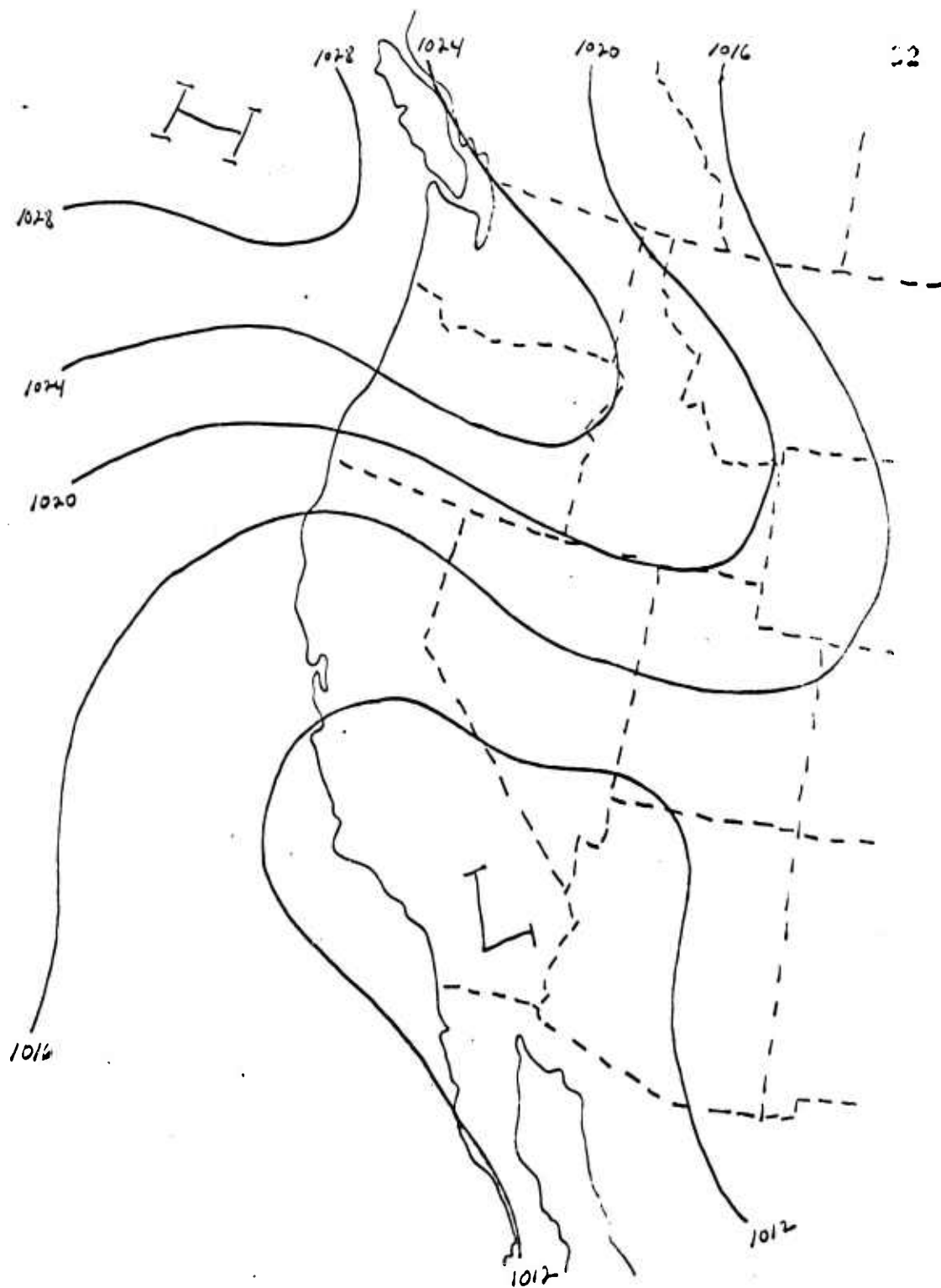


Figure 8. Pacific high pressure cell displaced inland (composite from NMC analysis of Class III weather map).

resulting in increased subsidence and a corresponding intensification and lowering of the subsidence inversion. The descending inversion confines the marine layer to an ever decreasing depth and may eliminate it altogether. The marine layer is, therefore, rapidly modified as it moves onshore and cannot reach Sacramento in spite of the advective effects of the light southwest winds of Class IIIA. As the intensifying inversion lowers, it descends below the level of the surrounding Coastal Mountains leaving only the narrow passage through the Carquinez Strait available for marine penetration into the Valley. This further reduces the extent of marine penetration inland. The northerly winds of Class IIIB sweep the Valley free of marine air, pushing it westward through the Carquinez Strait and out to sea.

The Class IIIA day is associated with a ridge from the central high pressure cell extending inland over Oregon and Northern California, creating higher than normal pressures to the north and east and balancing the usual onshore pressure gradient. Gradients in the interior Valley are weak or nonexistent. The existing pressure distribution causes weak southwesterly winds (from 210° - 250°) of less than or equal to 10 knots in the Valley.

Occasionally, a cell of high pressure will extend deep into Nevada completely reversing the onshore gradient

24

and creating the northerly winds (from 340° - 030°) of Class IIIB. At this time, the interior Valley gradient is directed from north to south. As the northerly flow descends the slopes of the Sierritas and Sierra Nevadas, it is warmed and dried adiabatically producing very hot, dry weather in the Valley.

Remembering the Class I associated north winds, it can be said that north winds produce warming in the Valley only if they are gradient induced (Class IIIB). If they are associated with a trough aloft (Class I), they produce cooling.

Aloft, a high pressure ridge overlies the area during the Class III period. During Class IIIA, flow aloft below 10,000 feet is light and variable as are the winds at the two levels on the television tower. During Class IIIB, flow aloft may be light and variable or quite well developed from the northwest, north, or northeast. Winds on the tower are again light. Class IIIA and IIIB will be designated by a "3" in the forecasting system (see column headed X_7 in Table II).

TABLE II

CLASSIFICATION SYSTEM

<u>Wind Direction</u>	<u>Custiness</u>	<u>Temperature</u>	<u>Class</u>	<u>X₇</u>
90-180-270° (south winds) ..	yes	>normal	IIA-C ..	1
		<normal	I ..	1
	no	>normal ...	IIIA or IIB	1
		<normal ...	I ..	1
270-360-90° (north winds) ..		>normal ...	IIIB	1
		<normal ...	I ..	1

*The parameter X₇ is defined by the respective discrete classes shown in the above table. Its purpose is to provide a continuous variable for use as a predictand.

CHAPTER V

THE FORECASTING TECHNIQUES

Now that a basic model describing the operation of the sea breeze-marine penetration has been established, it should be possible to use the model to develop an objective forecast system. Before the forecast system can be developed, however, a choice must be made as to which method of statistical analysis is best suited and most convenient for use. Three statistical techniques were examined before this choice was made. The following discussion will outline the advantages and disadvantages of each, leading to the selection of the method employed in this study.

Statistical Methods

In general, the problem of developing a statistical forecasting procedure requires determination of the functional relationship between a "predictand" (the weather variable which is to be predicted) and a number of "predictors" (the meteorological measurements believed to be related to the predictand at a previous time). Or, in functional notation, it is desired to determine

$$Y = f(X_1, X_2, X_3, \dots, X_i, \dots, X_n)$$

where $f(X_i)$ is not known.

The mathematically most satisfying method, linear multiple regression, requires an assumption that the relationship between the terms is linear, or can be made so by an appropriate transformation of the predictor variables. Since, in general, meteorological relationships are highly non-linear, and in this case are not known, a great deal of preliminary analysis would be required in order to determine the form of the relationship. Furthermore, the determination of the regression equation itself would then require exhaustive desk-computer analysis and/or the availability of electronic computing equipment. Finally, it has not been the general experience of other investigators that such techniques produce more satisfactory results than simple graphical methods (Panofsky, 1963).

Successive stratification is a relatively simple statistical method for analyzing data, especially non-linear data, wherein the investigator groups all of his data into distinct classifications. Herein lies the chief fault of the system. The investigator gradually works his way to a point where he has used all of the relevant classifications, yet there may still be some data remaining which does not fit any of these groupings. The problem, then, is what to do with the remaining data. If it is a relatively small portion of the sample, the temptation arises to neglect it as being so rare that it is not

particularly important in indicating how the predictand will react. However, it is just these rare combinations which may precede important meteorological phenomena that the investigator wishes to predict. On the other hand, if the portion of data is relatively large, the investigator is forced into either neglecting a large portion of his sample or devising new classifications.

Successive graphical regression involves the combination of successive pairs of predictors, each pair determining an estimate of the value of the predictand. When more than a single pair of predictors is used, the initial estimates are similarly paired, determining a new estimate of the value of the predictand in which four predictors have been combined. In functional notation this may be expressed as

$$Y = g_1\{g[f(X_1, X_2), f_1(X_3, X_4)], f_2(X_5, X_6)\} \dots$$

The advantages of this method are numerous. It is relatively simple and fast requiring no equipment other than pencil and graph paper. Unlike linear multiple regression, no assumption as to the nature of the relationship between terms is required. In fact, the data are used to determine the form of the relationship, thus eliminating the need for excessive preliminary analysis or involved calculations of the regression equation. Once the data have been plotted

and analyzed, an idea as to the usefulness of the predictors is available. If the isopleths on a given diagram are nearly horizontal or vertical, one of the predictors has no effect on the predictand. If the predictand is scattered randomly on the diagram, with little systematic trend, neither of the predictors on that particular diagram is useful. Other characteristics of the method include the effect of the order of combination of the predictors, that is, different combinations may yield different forecast values of the predictand. This is a disadvantage of the method. In general, these combinations which, on the basis of physical reasoning, seem to have a joint significance should, of course, be paired. However, while the meteorological validity of this initial relationship may be justified in this manner, the complexity of the secondary combinations generally defeats any attempt to analyze the relationships on the basis of a possible theoretical connection (Panofsky, 1963; Air Weather Service Manual, 1955). This was the method finally settled upon as being most suitable for this study.

Forecasting the Marine Penetration

Method. The first forecast attempted was the occurrence or non-occurrence of the marine penetration.

Using the basic ideas developed in the marine penetration model, six variables were chosen as predictors of the penetration. These variables, shown in Table III, were graphically combined using the successive graphical regression method.

TABLE III

MARINE PENETRATION INDEPENDENT VARIABLES

Pressure difference PDX-SFO	$\{x_1\}$	y_1		
Pressure difference RNO-SAC	$\{x_2\}$		y_4	
Inversion base pressure	$\{x_3\}$	y_2		y_5
SUU wind speed	$\{x_4\}$			
Pressure difference RBL-SAC	$\{x_5\}$	y_3		
24 hour 1000-700 mb thickness OAK	$\{x_6\}$			

The first pair of predictors chosen were the Portland, Oregon - San Francisco, California (PDX-SFO) and the Reno, Nevada - Sacramento, California (RNO-SAC) pressure differences. The variance of these predictors for the various classes may be found in Tables XIIA and B in the appendix. These predictors were chosen as being representative of the north-south and east-west pressure gradients respectively. As such, they are indicative of the presence or lack of a ridge in the Oregon-Nevada area. Positive values imply no marine penetration, while negative values indicate penetration. The combination of these variables yields the estimate of the strength of the

marine penetration designated Y_1 .

The second pair of predictors were the Oakland, California (OAK) inversion base pressure and the Fairfield, California (SUU) wind speed (sustained wind speed only, gusts are not taken into account). The variance of the Oakland inversion base pressure for the various classes may be found in Tables XIIA and B. The inversion base pressure represents the depth of the marine layer, while the Fairfield wind speed provides an indication of the proximity and rate of flow of the marine air as it penetrates through the Carquinez Strait and into the Sacramento River Delta area. The combination of these variables yields Y_2 .

The final pair of predictors were the Red Bluff, California - Sacramento, California (RBL-SAC) pressure difference and the 24 hour thickness change (1000-700 mb) as measured from the Oakland radiosonde observation. The Red Bluff - Sacramento pressure difference represents the interior Valley pressure gradient, nearly zero for Class III but negative for Class I, while the thickness change gives a measure of the cold air advection into the area providing an indication of the potential for trough development aloft and, therefore, of marine penetration. Combining these variables yields Y_3 . All data were collected from the 0300 hours PDT observation.

Initially, values of X_1 and X_2 were plotted on a scattergram. On this diagram, values of X_7 from Table II, Chapter IV were tabulated. The data were then smoothed by averaging groups of ten data points, and isopleths of X_7 were drawn. The isopleths, denoted by Y_1 , represent a preliminary estimate of X_7 . Similarly, the other predictors were combined; Y_2 represents an estimate of X_7 predicted from the graph with X_3 and X_4 as coordinates, and Y_3 an estimate of X_7 from X_5 and X_6 . Next, Y_1 and Y_3 were combined, as functions of four independent variables, to yield Y_4 .

The final graph, representing the combination of Y_2 and Y_4 , produced the final forecast of X_7 , denoted by Y_5 . Actual values of X_{1-7} and computed values of Y_{1-5} may be found in Table XIII in the appendix. Figures 9a-e are the forecasting graphs. To make a forecast, one merely determines the values for each of the initial predictors and enters these values on the appropriate graph to obtain Y_1 , Y_2 , and Y_3 . These values are used in the succeeding graphs to obtain Y_4 and Y_5 .

For values of Y_5 , the following scale was used to provide a best estimate of the three categories of marine influence--generally represented by the three classes of the marine penetration model.

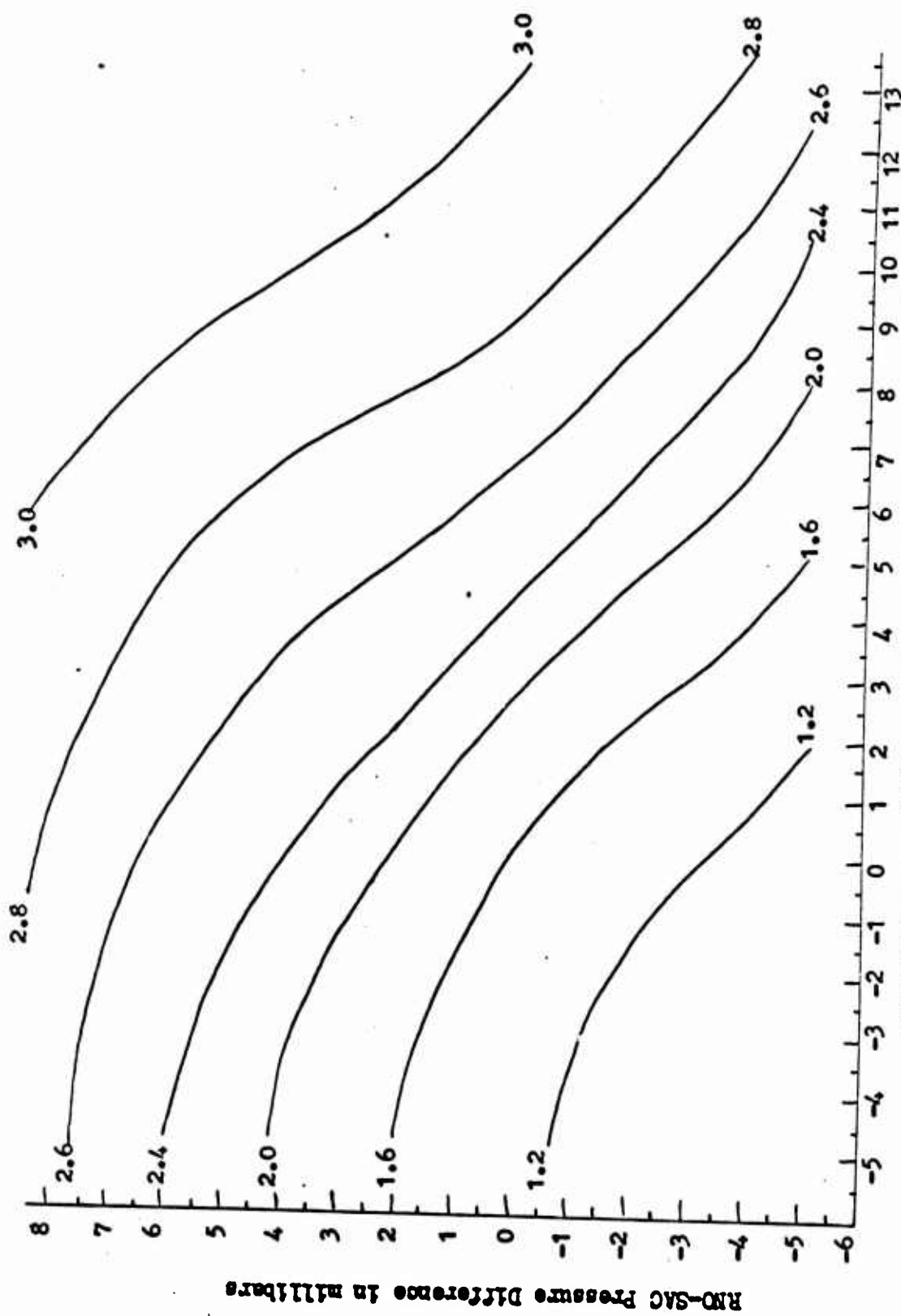
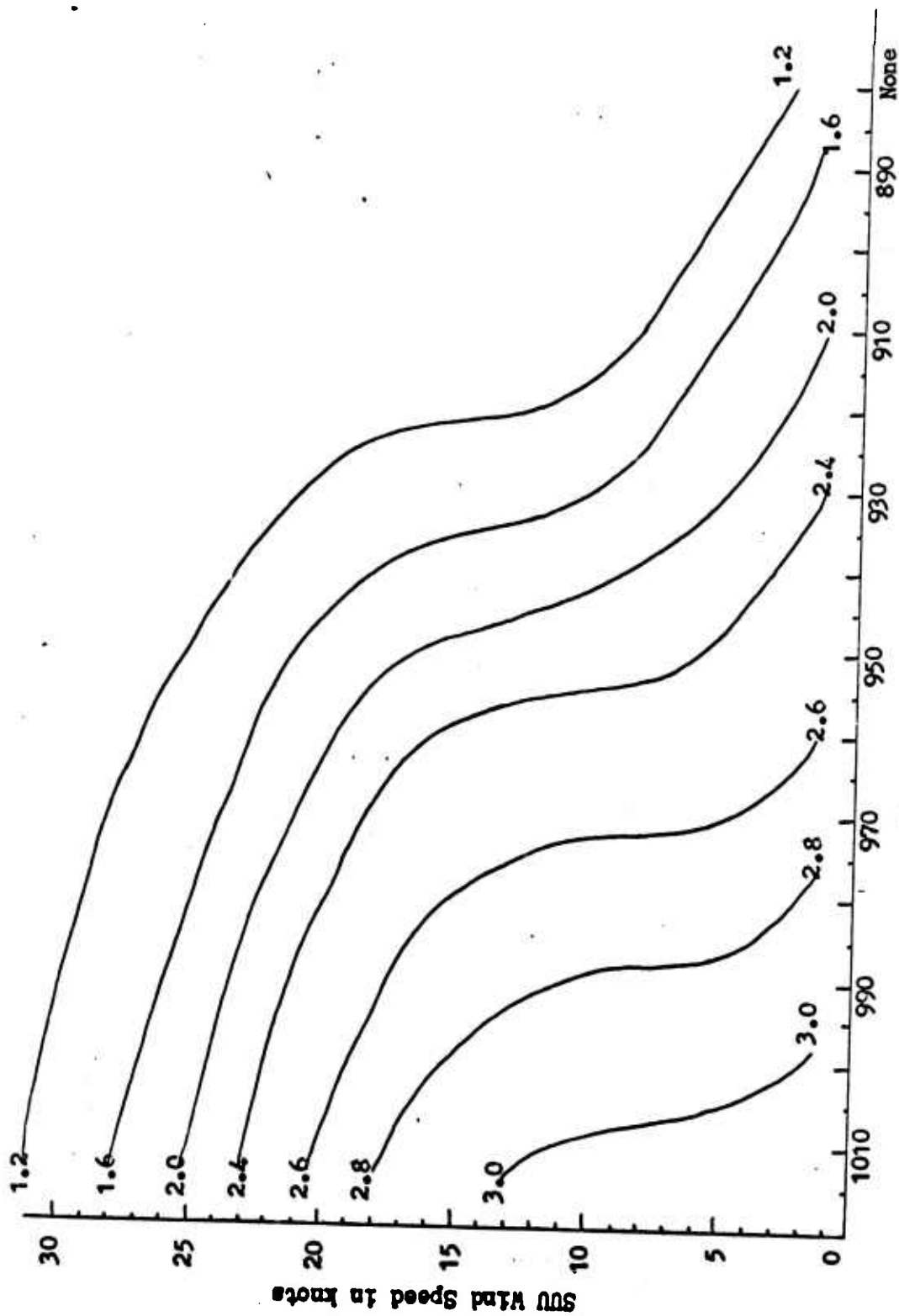


Figure 9a. Marine penetration forecast graph.



OAK Inversion Base Pressure in millibars

Figure 9b. Marine penetration forecast graph.

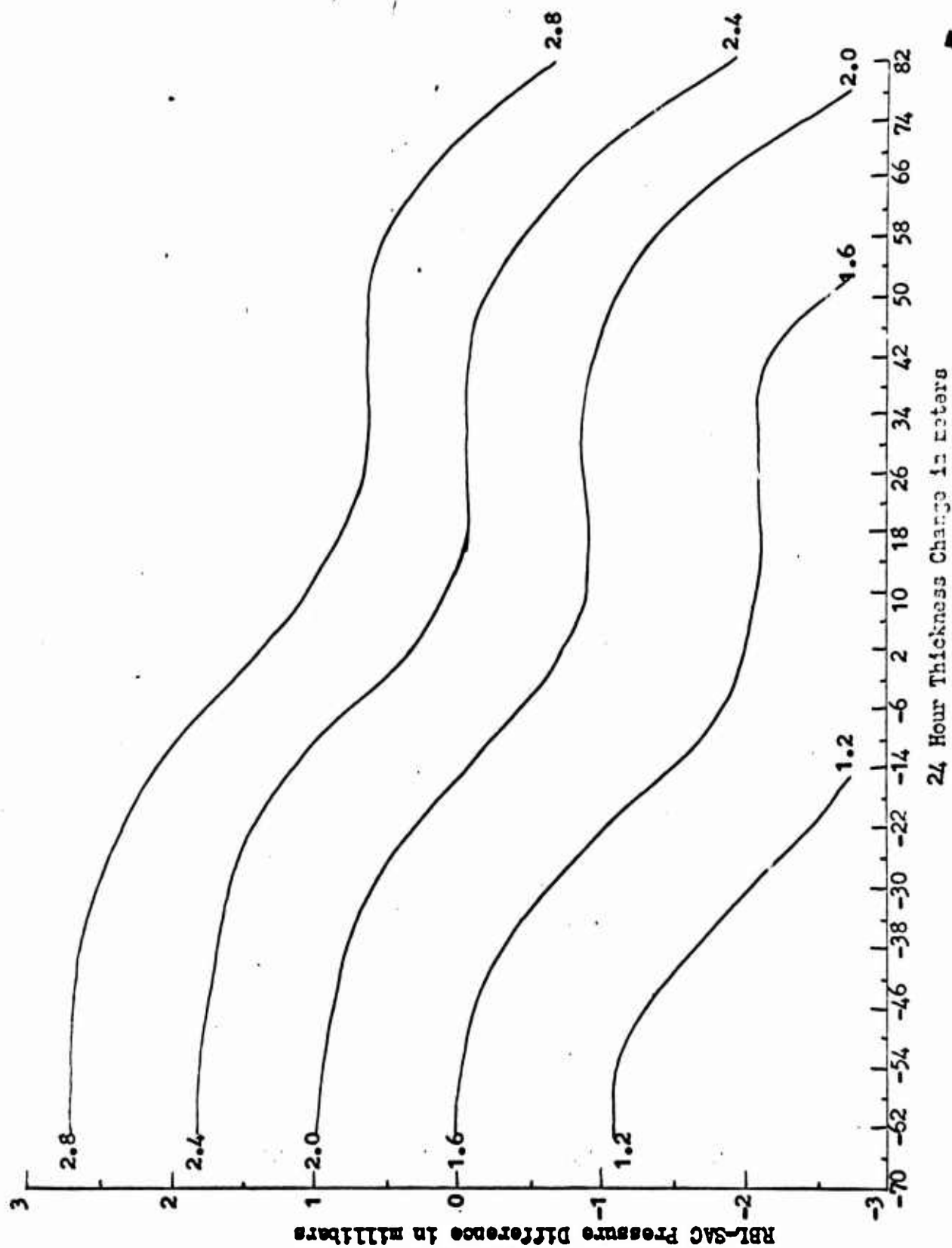


Figure 9c. Marine penetration forecast graph.

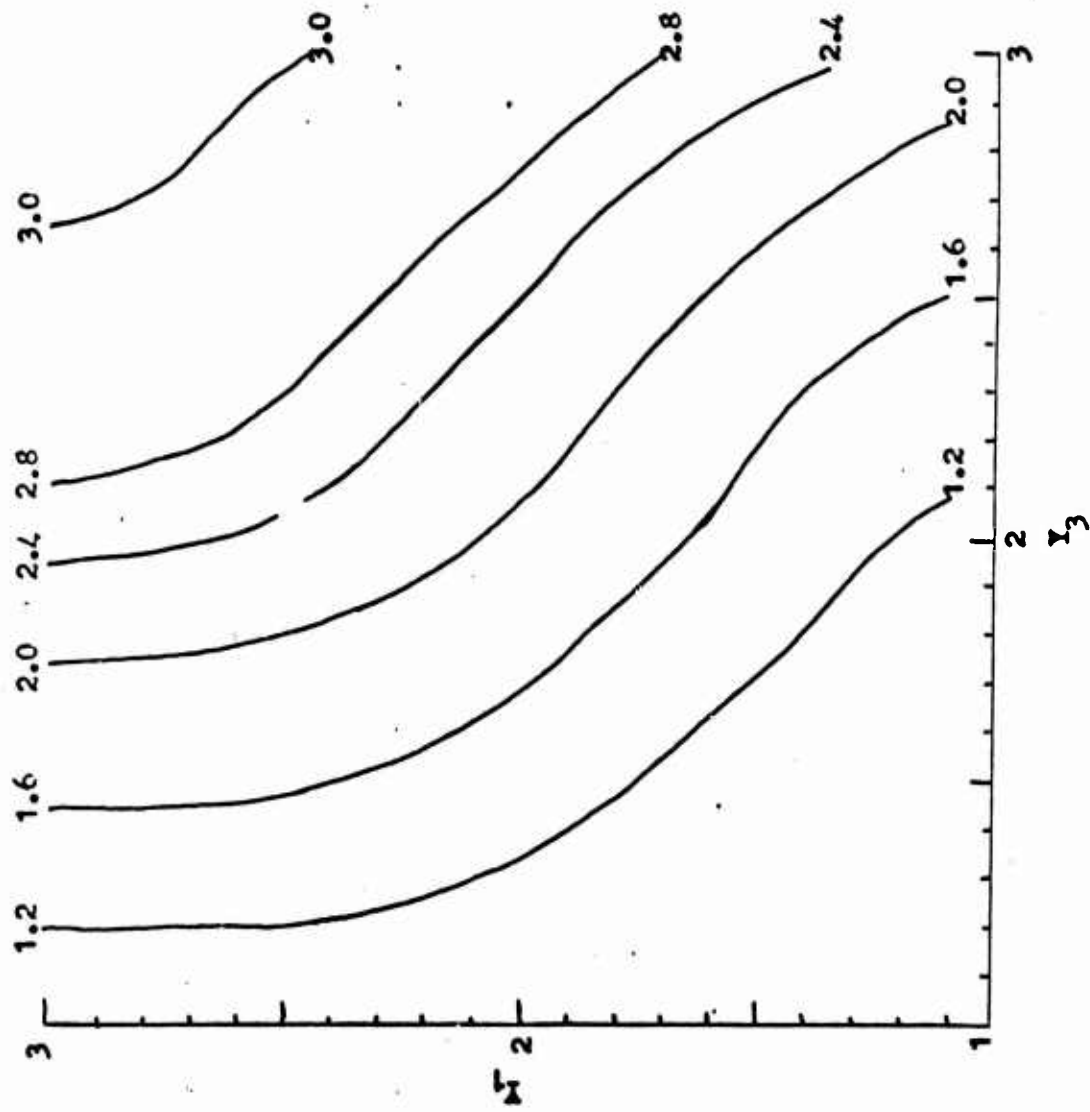


Figure 9d. Marine production forecast 5332a.

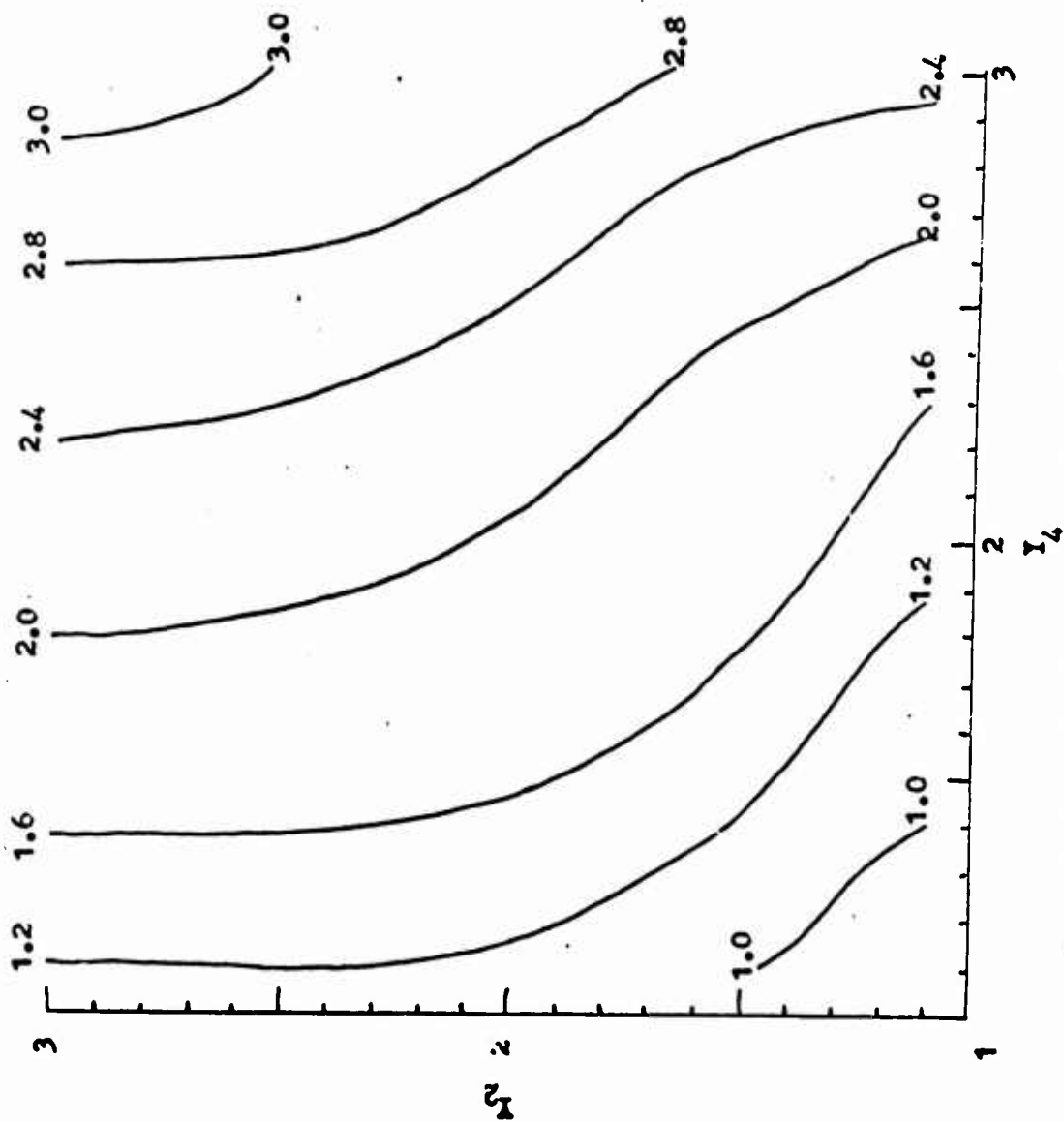


Figure 3c. Marine penetration forecast graph.

<u>Y_1</u>	<u>Marine Influence</u>	<u>Class</u>
1.0 - 1.6	Marine penetration	I
1.7 - 2.3	Sea breeze	IIA and C
2.4 - 3.0	Little or no marine influence	IIIA and B and IIB

Results. After the forecasting diagrams were constructed, two sets of data (the original set from 1963 and 1966 used to construct the graphs and an independent sample from 1964) were used to check the accuracy of the diagrams. The validity of the diagrams could thus be examined by comparing the results gained from using the dependent sample. Since the results, using the two sets of data, were not too dissimilar, it was assumed that the forecast diagrams were valid. In addition, by using both the dependent data as well as an independent sample, a total of three years data were used in determining the validity of the diagrams.

Looking first at the dependent data sample, several things can be determined from Table XIII. Y_1 is a highly variable predictor subject to rapid and sudden changes between predictions of no marine penetration and marine penetration. It is, therefore, very useful in predicting the change from one class to the other. Similarly, Y_2 is also highly variable and, therefore, a good forecaster of change. Y_3 ,

on the other hand, is extremely conservative. For the most part, values of Y_3 tend to center about an X_7 value of "2".

Table IVA is a comparison of forecast occurrences of Y_3 to the actual occurrence of X_7 based on the results shown in Table XIII. As can be seen, there were 46 actual cases of Class I, 17 of Class II, and 72 of Class III. Y_1 and Y_2 were successful in forecasting 50% or more of the occurrences of Class I and III. However, they were quite unsuccessful in forecasting Class II. Y_3 , on the other hand, was correct more than 50% of the time in forecasting Class II although less accurate in forecasting the other classes. It is clear, then, that Y_3 is the best forecaster of the sea breeze and is needed if such a forecast is to be made.

The combination of Y_1 and Y_3 yielded an immediate improvement in the forecasting of both Class I and III and also increased the accuracy of the Y_1 forecast of Class II; however, there was a corresponding decrease of the accuracy of Y_3 in forecasting Class II. The combination of Y_2 and Y_4 again brought an improvement to the forecast of Class I, a slight loss of accuracy in the forecast of Class III, and no change in the accuracy of the forecast of Class II. The overall accuracy after the addition of Y_2 to Y_4 was, however, increased. From Table IVA, it appears as though each predictor pair contributed significantly to the improvement of the forecast.

TABLE IVA

COMPARISON OF FORECAST OCCURRENCES OF Y_3 TO ACTUAL
OCCURRENCES OF X_7 DEPENDENT DATA

X_7	No. of actual occurrences	Y_1 correct forecasts	Y_2 correct forecasts	Y_3 correct forecasts	Y_4 correct forecasts	Y_5 correct forecasts
1	46	25	23	11	28	33
2	17	5	4	9	7	7
3	72	60	35	41	61	59
Sum	135	90	82	61	96	99

TABLE IVB

COMPARISON OF FORECAST OCCURRENCES OF Y_3 TO ACTUAL
OCCURRENCES OF X_7 INDEPENDENT DATA

X_7	No. of actual occurrences	Y_1 correct forecasts	Y_2 correct forecasts	Y_3 correct forecasts	Y_4 correct forecasts	Y_5 correct forecasts
1	14	10	10	9	10	10
2	16	5	2	15	10	12
3	30	23	25	12	21	23
Sum	60	38	37	36	41	45

Both the per cent correct and the skill score were computed as shown in Table V. Briefly, the results were: 73% correct and a skill score of .56.

The independent sample of 60 cases from July and August 1964 was examined. The same procedures were followed with similar results (see Table IVB). Again, Y_3 correctly forecast Class II (in fact it hit a phenomenal 15 out of 16 of the Class II occurrences). Y_1 and Y_2 were again better than 50% in forecasting Classes I and III. Y_4 showed a significant improvement over Y_1 in the Class II forecast, while again the Class III forecast suffered a drop in accuracy. Y_3 produced a more accurate forecast on the whole than any of the other forecasts, scoring 37 out of 48 forecasts correct.

The contingency table shown in Table VI yielded a per cent correct of 70% while the skill score was .61. This apparent "improvement" over the dependent data is believed to be a non-significant variation; a chi-square test of the difference in scores indicated this to be the case.¹ Table XIV in the appendix shows the actual data for

¹While the validity of statistical tests of this kind on meteorological data is somewhat uncertain, the results in this case support the intuitive feeling.

TABLE V
MARINE PENETRATION FORECAST DEPENDENT
DATA CONTINGENCY TABLE*

FORECAST					
	1.0- 1.6	1.7- 2.3	2.4- 3.0		
OBSERVED	1	33 (13.3)	10	2	45
	2	3	7 (3.4)	7	17
	3	4	10	59 (36.8)	73
		40	27	68	135

Per Cent Correct: $\frac{99}{135} \times 100 = 73\%$

Skill Score: $\frac{\text{Number Correct} - \text{Number Expected Correct}}{\text{Total} - \text{Number Expected Correct}}$

$$\frac{99 - 34}{135 - 34} = \frac{65}{101} = .64$$

*On all contingency tables, the numbers in parentheses in a box are the number of cases which would occur by chance in that box, based on the marginal totals of the tables. These are the "number expected correct" in the skill score.

TABLE VI

MARINE PENETRATION FORECAST INDEPENDENT
DATA CONTINGENCY TABLE
FORECAST

OBSERVED		1.0- 1.5	1.7- 2.3	2.4- 3.0	
	1	10 (2.8)	3	0	13
	2	2	12 (5.9)	2	16
	3	1	7	23 (13.0)	31
		13	22	25	60

Per Cent Correct: $\frac{43}{60} \times 100 = 71\%$

Skill Score: $\frac{43}{60} - \frac{21.7}{30} = \frac{21.3}{30} = .61$

X_{1-7} and Y_{1-5} for the independent sample.

Forecasting the Maximum Temperature

Method. The forecasting diagrams for determining the maximum temperature were developed in the same manner as those used in forecasting the marine penetration. In addition, essentially the same predictors were used, although in somewhat different combinations and with one change. Here, instead of using the scale value of X_7 (1, 2, or 3), the actual maximum temperature that occurred on the day of the observation was plotted on the scattergram and analyzed.

The independent variables used are shown in Table VII. As can be seen, the initial pair of predictors, the Portland - San Francisco and Reno - Sacramento pressure differences, yielded Z_1 . The Oakland inversion base pressure and the Red Bluff - Sacramento pressure difference were combined on the second diagram to yield Z_2 . Finally, the Fairfield wind speed and the 850 mb temperature (reduced dry adiabatically to the surface) from the Oakland radiosonde observation were combined to yield Z_3 . Again, all data were taken from the 0500 hours PDT observation.

The 850 mb temperature replaced the 1000-700 mb 24 hour thickness change because on most days it seemed to correlate quite well with the observed maximum temperature

in Sacramento. On most days, surface heating occurs until the temperature reaches that of the 850 mb level. Any further heating produces convective mixing which spreads the heat through a deep layer of the atmosphere retarding further heating of the surface layers.

TABLE VII

MAXIMUM TEMPERATURE INDEPENDENT VARIABLES

Pressure difference PDX-SFO	$\{X_1\}$	Z_1	
Pressure difference RNO-SAC	$\{X_2\}$		Z_4
Inversion base pressure OAK	$\{X_3\}$	Z_2	
Pressure difference RBL-SAC	$\{X_5\}$		
SUU wind speed	$\{X_4\}$		Z_3
850 mb temperature	$\{X_8\}$	Z_3	

The values of Z_1 and Z_2 were combined to yield Z_4 . Z_3 and Z_4 were combined to yield Z_5 , the forecast of X_7 . The forecasting diagrams are shown in Figures 10a-e, while the actual values of X_{1-5} , X_8 , and the computed values of Z_{1-5} are shown in Table XV in the appendix.

Results. Again, as with the marine penetration forecast, two sets of data were used to check the accuracy of the diagrams; however, this time the independent data came from 1958. From looking at Table XV, it may be determined that Z_1 and Z_3 are the more variable parameters,

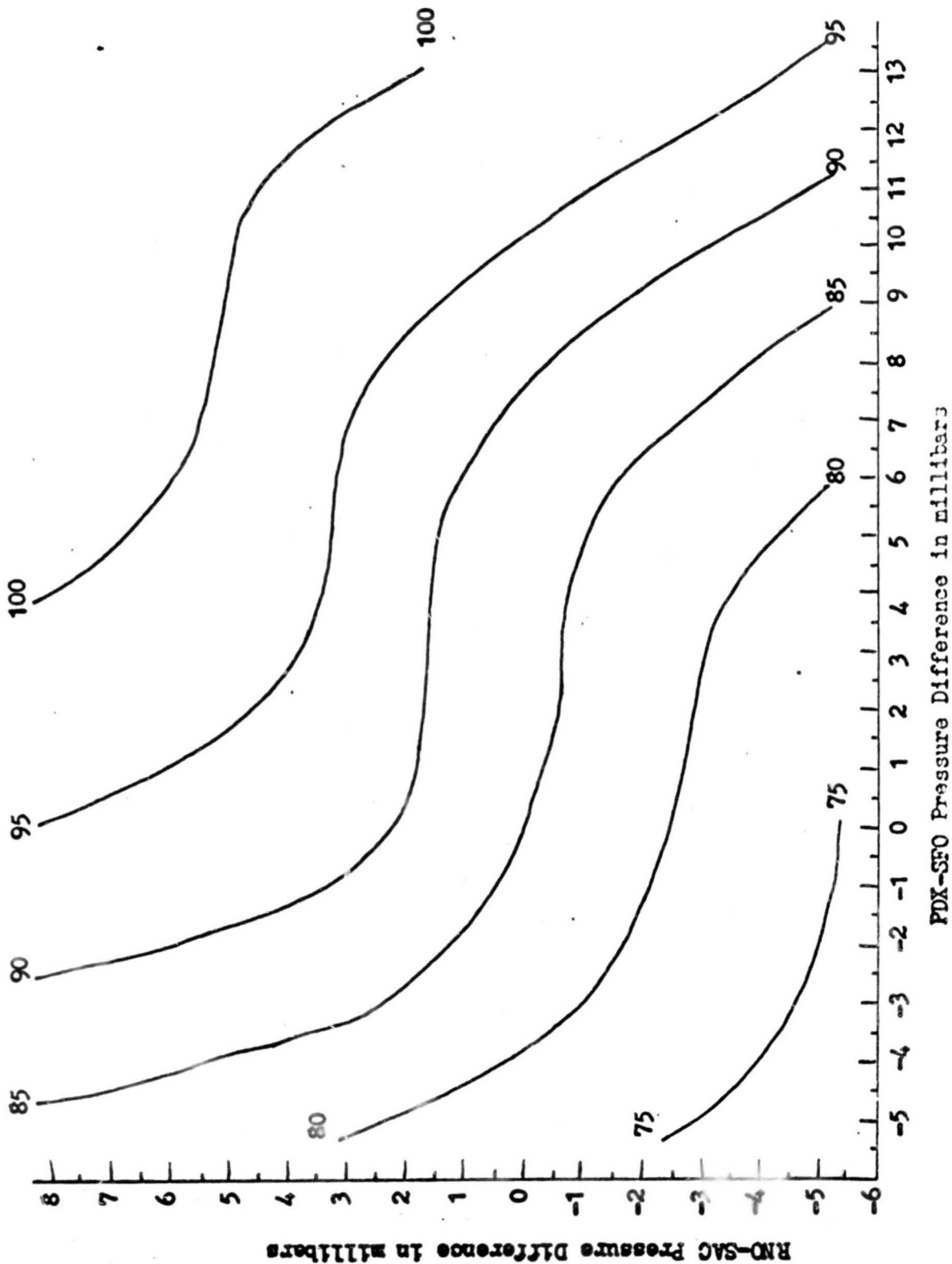
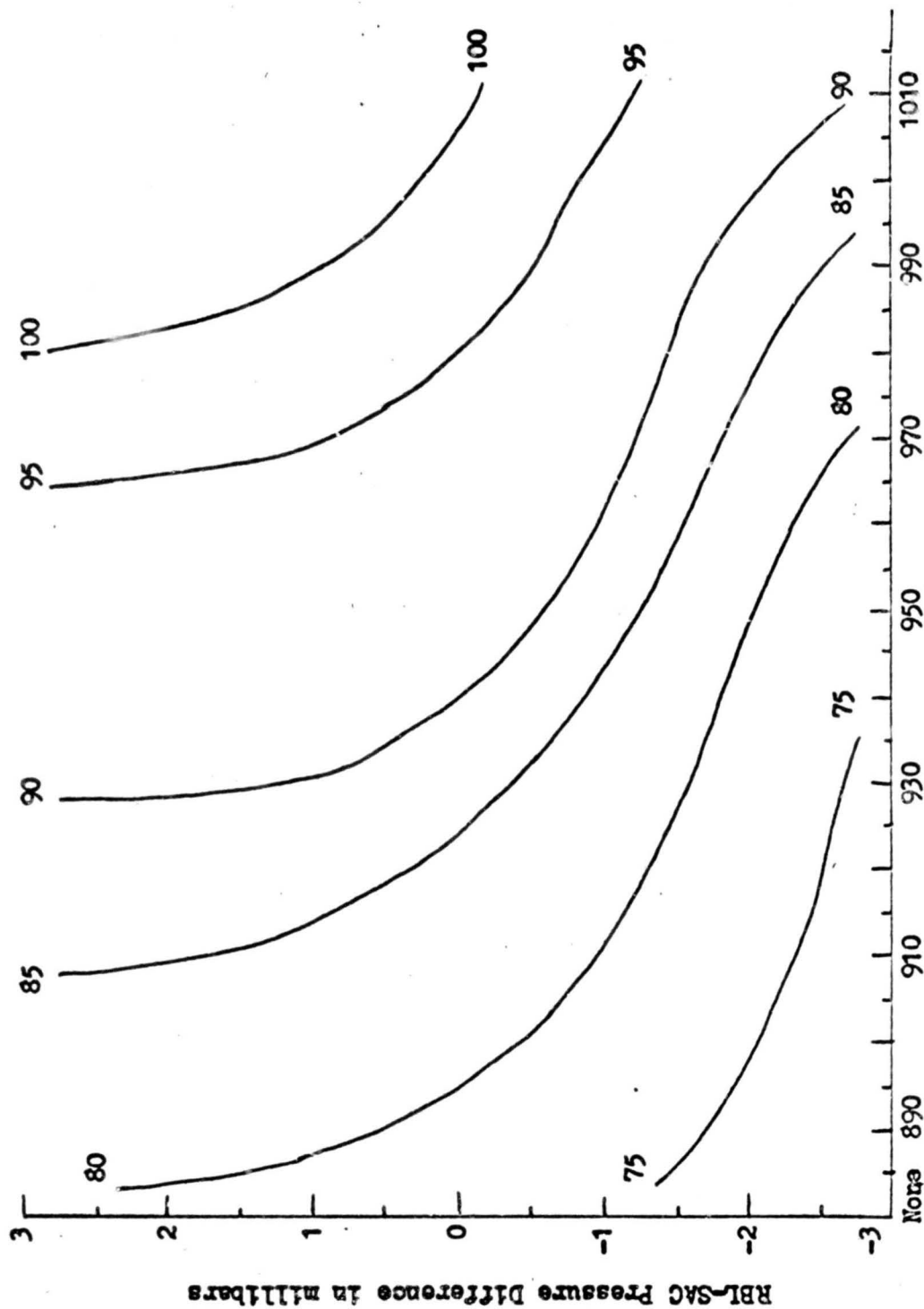


Figure 10a. Maximum temperature forecast graph.



OAK Inversion Base Pressure in millibars

Figure 1Cb. Maximum temperature forecast graph.

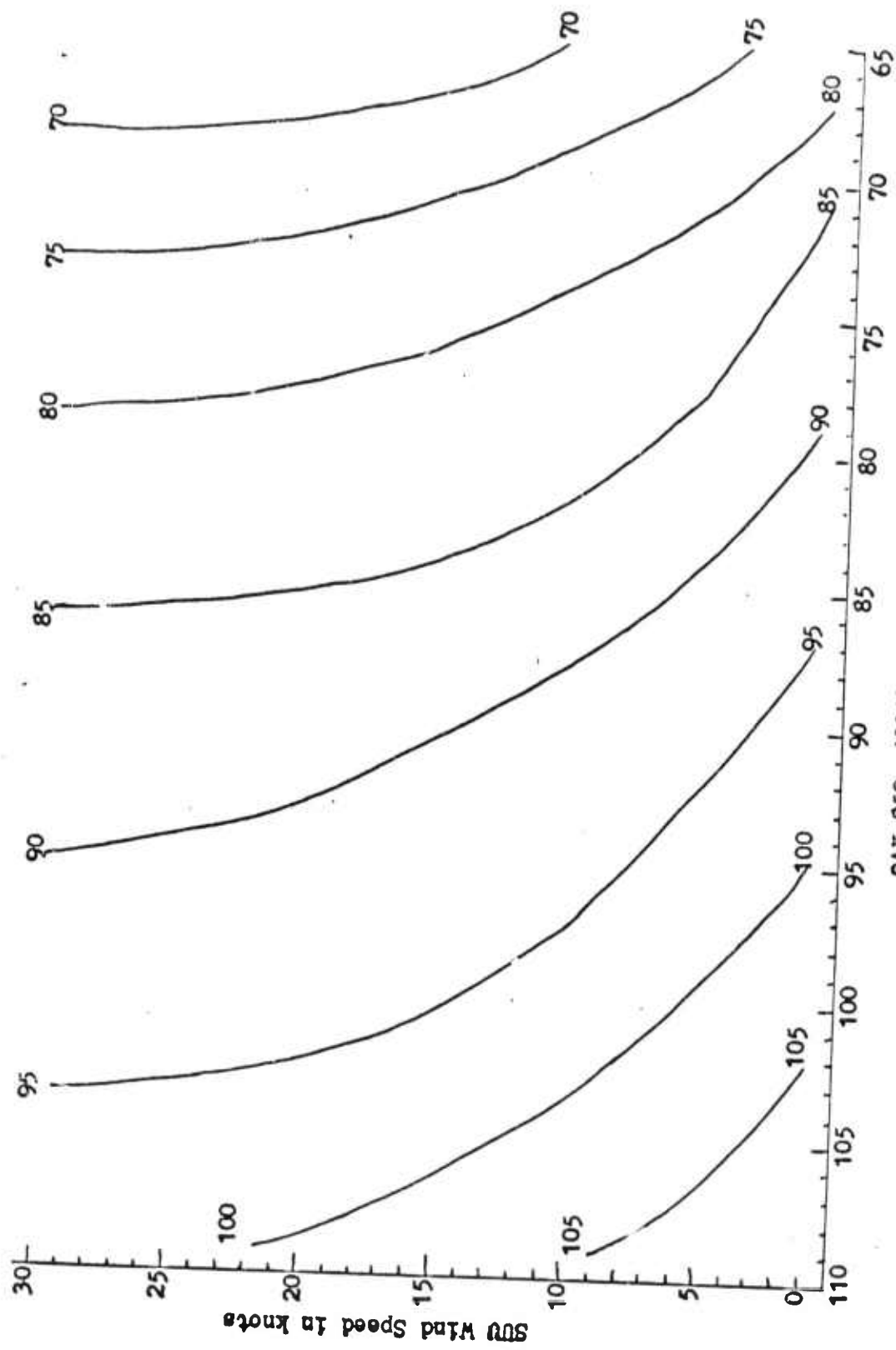


Figure 13c. Maximum temperature forecast 82.5.

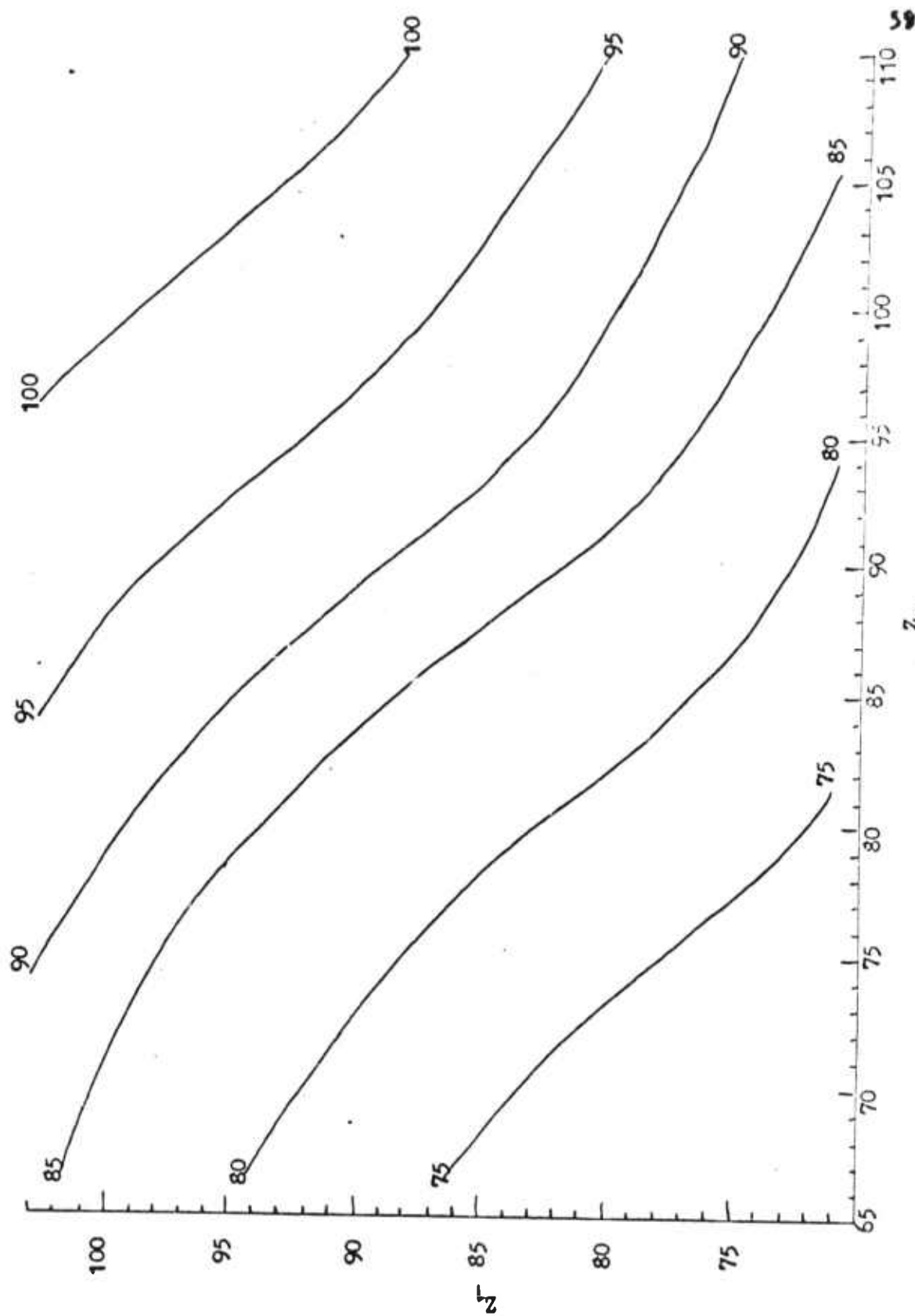


Figure 10d. Maximum temperature forecast graph.

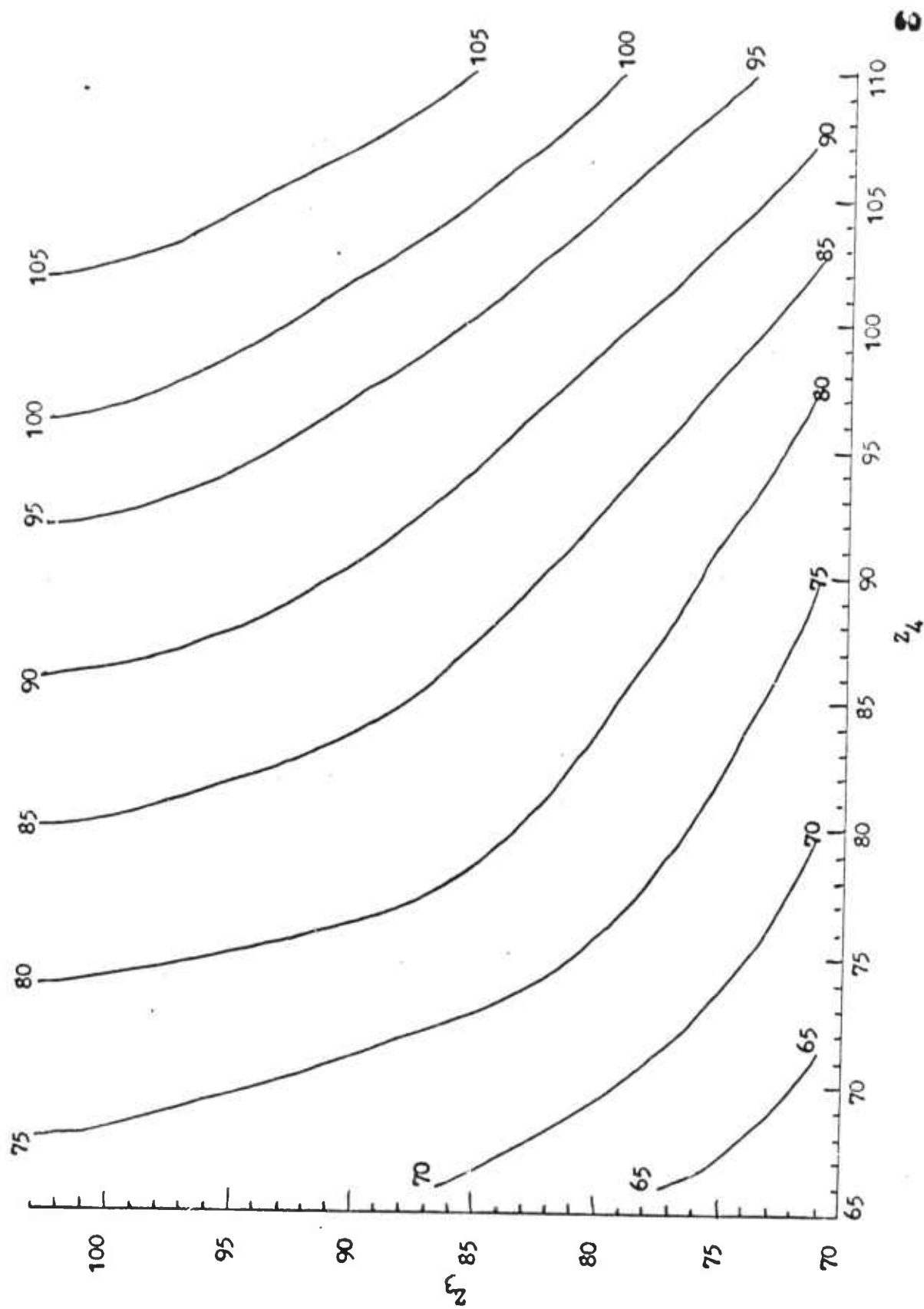


Figure 10e. Maximum temperature forecast graph.

while Z_2 is slightly more conservative. Hence, it would be expected that Z_1 and Z_3 would respond much more quickly to the change from Class I to Class III, while Z_2 would act as a moderating influence.

For verification purposes, the temperatures were divided into four class intervals: less than 80°F , $80-89^{\circ}\text{F}$, $90-99^{\circ}\text{F}$, and greater than or equal to 100°F .

Looking first at the dependent data, Table VIIIA is a comparison of forecast occurrences of Z_3 to the actual occurrence of X_7 based on the results in Table XV. There were 20 actual cases of temperatures less than 80°F , 43 of temperatures from $80-89^{\circ}\text{F}$, 60 of temperatures from $90-99^{\circ}\text{F}$, and 26 of temperatures greater than or equal to 100°F . Z_{1-3} were successful in forecasting correctly over 50% of the time for the two class intervals $80-89^{\circ}\text{F}$ and $90-99^{\circ}\text{F}$, but were much less successful in forecasting the other two intervals. The combination of Z_1 and Z_2 to yield Z_4 provided an improvement in the forecast of the class interval greater than or equal to 100°F , and yielded little change in the other intervals. The total number correct for Z_4 was greater than for Z_{1-3} .

The combination of Z_3 and Z_4 to yield Z_5 provided notable improvement in the forecast of the class intervals less than 80°F , $80-89^{\circ}\text{F}$, and tremendous improvement of the

TABLE VIIIA

COMPARISON OF FORECAST OCCURRENCES OF Z_5 TO ACTUAL
OCCURRENCES OF X_7 DEPENDENT DATA

X_7	No. of actual occurrences	Z_1 correct forecasts	Z_2 correct forecasts	Z_3 correct forecasts	Z_4 correct forecasts	Z_5 correct forecasts
80	20	3	4	2	4	7
80-89	43	30	22	29	30	33
90-99	80	70	65	69	70	65
100	26	4	9	6	7	20
Sum	169	105	100	106	111	125

TABLE VIIIB

COMPARISON OF FORECAST OCCURRENCES OF Z_5 TO ACTUAL
OCCURRENCES OF X_7 INDEPENDENT DATA

X_7	No. of actual occurrences	Z_1 correct forecasts	Z_2 correct forecasts	Z_3 correct forecasts	Z_4 correct forecasts	Z_5 correct forecasts
80	1	1	1	1	1	1
80-89	12	5	2	4	1	2
90-99	27	19	20	24	22	13
100	6	2	6	4	4	6
Sum	46	27	29	33	23	27

greater than or equal to 100°F interval. There was a slight decline in the accuracy of the $90-99^{\circ}\text{F}$ interval; however, the total number of correct forecasts was significantly better than any of the other forecasts of Z . Hence, it appears as though each predictor pair is contributing to the improvement of the forecast.

Both the per cent correct and the skill score were computed as shown in Table IX. The results were 67% correct and a skill score of .50.

The independent sample of 46 cases from August and September 1938 was examined. The results were not as favorable as they were for the dependent sample (see Table VIII B). Z_5 did not produce the best forecasts as the total number correct for Z_5 was only 27, and Z_3 produced a total number correct of 33. The reason for this is thought to lie in the relatively small size of the sample and the fact that only 13 of the 46 cases fell in the two class intervals less than 80°F and $80-89^{\circ}\text{F}$. Nevertheless, the skill score and per cent correct, which were .32 and 59% respectively, were quite similar to those computed for the dependent data (see Table X). There was a slight reduction in accuracy from the dependent data; however, the differences in scores were non-significant when tested by the chi-square test (see footnote 1, page 51). Table XVI in the appendix gives actual values of X_{1-5} , X_8 , and computed values of Z_{1-5} for the independent sample.

TABLE 1A
 MAXIMUM TEMPERATURE FORECAST DEPENDENT
 DATA CONTINGENCY TABLE

FORECAST						
	100	90-99	80-89	80		
OBSERVED	100	20 (5.1)	6	0	0	26
	90-99	13	63 (39.2)	2	0	80
	80-89	0	11	31 (11.4)	3	45
	80	0	1	10	7 (1.1)	18
		33	83	43	10	169

Per Cent Correct: $\frac{113}{169} \times 100 = 67\%$

Skill Score: $\frac{113 - 37}{169 - 37} = \frac{76}{132} = .58$

TABLE X

MAXIMUM TEMPERATURE FORECAST INDEPENDENT
DATA CONTINGENCY TABLE

OBSERVED	FORECAST				
	100	90-99	80-79	80	
	100	6 (2.1)	0	0	6
	90-99	9	13 (14.7)	0	27
	80-79	1	7	2 (0.7)	11
	80	0	0	1 (0.1)	2
	16	23	3	2	46

Per Cent Correct: $\frac{27}{46} \times 100 = 59\%$

Skill Score: $\frac{27}{46} - \frac{13}{46} = \frac{14}{46} = .32$

CHAPTER VI

CONCLUSION

Essentially, the high degree of skill displayed by the marine penetration and maximum temperature forecast techniques justifies acceptance of the marine penetration model described in Chapter IV.

With respect to the model, it seems as though the Pacific high pressure cell is definitely connected with the occurrence of the marine penetration, as witnessed by the high degree of accuracy of the Y_1 forecast of Class I and Class III. On the other hand, the development of the thermal trough in the interior Valley of California influences the development of the sea breeze as witnessed by the accuracy of Y_2 in forecasting Class II.

The isotherm pattern shown in Figure 8 clearly indicates the movement of cool marine air from the ocean into the Bay and from the Bay into the Central Valley through the Carquinez Strait. The development of a jet-like core of cool air through the Strait is a convincing picture of the marine penetration.

The depth of the marine layer is also dominant in the marine penetration. It is evident, that on days when the temperature inversion is low and the marine layer shallow, no serious penetration will occur. With a deep marine

layer, penetration is not only possible, but probable.

It seems evident that the basic idea of the model is correct, although all of the variables may not work for every case. When they do not, the strength of the penetration is reduced. Indeed, one would not expect a harmonious working of every variable for every penetration. Clearly, though, observation of the variables set forth should give some idea of the occurrence or non-occurrence of the marine penetration. The overall usefulness of this forecasting system can only be proven by actual in-station use. It was toward this end that the study was undertaken, and hopefully, it is this end which the study will fill.

REFERENCES

- Byers, A. R., 1931, Characteristic Weather Phenomena of California. MIT Meteorol. Papers, Vol. 1, no. 2. Cambridge, Mass. 34 pp.
- Department of the Air Force, 1955. Some Techniques for Deriving Objective Forecasting Aids and Methods, ANSM 105-40 (REV). 51 pp.
- Edinger, J. A., 1959, Changes in the depth of the marine layer over the Los Angeles basin. J. Meteorol. 40(6): 219-226.
- Fosberg, M. A., and M. J. Schroeder, 1966. Marine air penetration in Central California. J. Meteorol. 5(5): 573-589.
- Harman, W. E., 1960. An objective method for forecasting the maximum temperature at Sacramento, California. In: Forecasting Maximum and Minimum Temperature, Forecasting Guide Number 4, United States Department of Commerce, Weather Bureau, 59 pp.
- Haurwitz, B., 1947. Comments on the sea-breeze circulation. J. Meteorol. 4(1): 1-8.
- Kaupar, E. K., 1960. The zone of discontinuity between the land and sea breezes and its importance to southern California air-pollution studies. Bull. Am. Meteorol. Society. 41(8): 410-422.
- Lowry, W. P., 1959. Energy budgets of several environments under sea-breeze advection in western Oregon. J. Meteorol. 16(3): 299-311.
- Meiburger, M., D. S. Johnson and C. W. Chien, 1961. Studies of the Structure of the Atmosphere Over the Eastern Pacific Ocean in Summer. U. of Calif., Berkeley, 98 pp.
- Panofsky, H. A., and G. W. Brier, 1963. Some Applications of Statistics to Meteorology. The Pennsylvania State University, University Park, Pennsylvania, 224 pp.

- Patton, C. P., 1956. Climatology of Summer Fogs in San Francisco Bay Area. U. of Calif., Berkeley, 200 pp.
- Root, H. E., 1960. San Francisco, the air conditioned city. Weatherwise. 13(2): 47-54.
- Riehl, H., 1954. Tropical Meteorology. McGraw Hill Book Company, Inc., New York, 392 pp.
- Schmidt, E. K., 1947. An elementary theory of the land and sea-breeze circulation. J. Meteorol. 4(1): 9-15.
- Schultz, H., N. B. Akesson, and W. E. Yates, 1961. The delayed sea breeze in the Sacramento Valley and the resulting favorable condition for application of pesticides. Bull. Am. Meteorol. Society. 42(10): 679-687.
- Snclair, P. C., 1961. Forecasting Summer-Time Maximum Temperatures at McClellan Air Force Base. Station Forecast Manual, 8 pp. (unpublished)
- United States Department of Commerce, 1964. Climatic Summary of the United States - Supplement for 1951 through 1960 - California. United States Government Printing Office, Washington, D. C., 216 pp.
- Wallington, C. W., 1961. Meteorology for Glider Pilots. Unwin Brothers Ltd., London, 284 pp.
- Williams, W. A., and R. E. DeMandel, 1966. Land-Sea Boundary Effects on Small Scale Circulations. San Jose State College Meteorology Department Research Report, 97 pp.

APPENDIX

TABLE XIA

AVERAGE PRESSURE OF INVERSION BASE (OAK)
AND PRESSURE DIFFERENCES AT 0500
PDT BASED ON 92 CASES IN 1966

Pressure Differences

<u>Class</u>	<u>Inv Base Pres</u>	<u>PDX- SFO</u>	<u>RNO- SAC</u>	<u>RRL- SAC</u>	<u># of Cases</u>
IIIA	982 mb	5.3 mb	4.1 mb	.2 mb	15
IIIB	993	7.9	5.1	1.4	10
IIA	965	3.3	2.4	-.5	4
IIB	978	3.8	3.8	.1	29
IIC	973	1.3	1.5	-.2	12
I	927	-.1	-.7	-.5	22

TABLE XIB

AVERAGE PRESSURE OF INVERSION BASE (OAK)
AND PRESSURE DIFFERENCES AT 1700
PDT BASED ON 92 CASES IN 1966

Pressure Differences

<u>Class</u>	<u>Inv Base Pres</u>	<u>PDX- SFO</u>	<u>RNO- SAC</u>	<u>RRL- SAC</u>	<u># of Cases</u>
IIIA	997 mb	3.9 mb	2.4 mb	-1.0	15
IIIB	1001	7.3	3.8	.1	10
IIA	985	3.4	1.7	-1.5	4
IIB	987	2.8	2.5	-1.3	29
IIC	976	-.2	-.3	-1.9	12
I	924	-1.1	-2.1	-1.5	22

TABLE XI A

RANGE OF THE PRESSURE
OF THE INVERSION BASE (OAK) AND
PRESSURE DIFFERENCES AT 0500 PDT
BASED ON 92 CASES IN 1966

<u>Class</u>	<u>Inv Base Pres</u>		<u>PDX- SFO</u>		<u>RNO- SAC</u>		<u>RBL- SAC</u>	
	<u>High</u>	<u>Low</u>	<u>High</u>	<u>Low</u>	<u>High</u>	<u>Low</u>	<u>High</u>	<u>Low</u>
IIIA	940	Sfc	10.2	1.4	6.6	.8	1.1	-.6
IIIB	960	Sfc	13.2	3.6	10.6	.6	3.6	.3
IIA	930	990	5.9	1.4	3.9	.8	-.1	-1.0
IIB	940	Sfc	7.7	-1.4	7.9	1.2	.7	-.9
IIC	940	1000	6.1	-5.3	3.4	-1.5	.6	-1.1
I	850	960	8.7	-2.8	4.1	-5.4	1.1	-2.1

TABLE XI B

RANGE OF THE PRESSURE
OF THE INVERSION BASE (OAK) AND
PRESSURE DIFFERENCES AT 1700 PDT
BASED ON 92 CASES IN 1966

<u>Class</u>	<u>Inv Base Pres</u>		<u>PDX- SFO</u>		<u>RNO- SAC</u>		<u>RBL- SAC</u>	
	<u>High</u>	<u>Low</u>	<u>High</u>	<u>Low</u>	<u>High</u>	<u>Low</u>	<u>High</u>	<u>Low</u>
IIIA	980	Sfc	8.3	-.1	5.0	.2	-.1	-1.9
IIIB	980	Sfc	10.9	1.3	10.3	-.7	1.3	-1.2
IIA	970	1000	6.1	.1	3.5	-.7	-1.3	-1.8
IIB	960	1000	7.6	-2.3	6.1	-1.1	-.6	-2.2
IIC	900	Sfc	4.8	-3.3	2.8	-2.5	-.8	-3.6
I	None	980	6.3	-5.2	1.8	-4.6	-.2	-3.0

TABLE XIII (continued)

Serial No.	X	Y	X	Y	X	Y	X	Y	X	Y	X	Y	X	Y	X	Y	X	Y
25	2.9	1.6	1	1	14	1.8	-	1.8	-15	1.6	1.3	1.3	-	1.3	-	1.3	-	1.3
26	4.6	1.6	1	1	3	2.4	-	1.6	-41	1.7	1.2	1.3	-	1.2	-	1.2	-	1.3
27	6.1	2.8	3	3	7	2.7	-	2.7	57	2.7	2.7	3.0	-	3.0	-	3.0	-	3.0
28	8.2	2.9	3	3	4	2.9	-	2.9	23	2.3	2.3	2.9	-	2.9	-	2.9	-	2.9
29	5.6	2.8	2	2	8	2.9	-	2.9	22	2.3	2.3	2.9	-	2.9	-	2.9	-	2.9
30	-2.6	1.6	1	1	19	1.4	-	1.4	-46	1.2	1.2	1.0	-	1.0	-	1.0	-	1.0
31	5.5	2.8	3	3	8	2.7	-	2.7	70	2.7	2.7	3.0	-	3.0	-	3.0	-	3.0
32	-	2.7	3	3	16	2.4	-	2.4	-34	1.5	1.5	1.7	-	1.7	-	1.7	-	1.7
33	-	2.7	3	3	13	2.4	-	2.4	-	-	-	-	-	-	-	-	-	-
34	5.2	2.8	2	2	4	2.6	-	2.6	-	-	-	-	-	-	-	-	-	-
35	-	2.7	1	1	18	1.7	-	1.7	-3	2.0	2.0	1.8	-	1.8	-	1.8	-	1.8
36	1.7	2.4	3	3	12	2.2	-	2.2	-8	2.2	2.2	2.8	-	2.8	-	2.8	-	2.8
37	6.7	2.8	3	3	14	2.2	-	2.2	-4	2.2	2.2	2.8	-	2.8	-	2.8	-	2.8
38	3.9	2.6	1	1	15	2.5	-	2.5	-8	2.3	2.3	2.9	-	2.9	-	2.9	-	2.9
39	1.3	1.8	1	1	14	2.5	-	2.5	-35	1.9	1.9	1.8	-	1.8	-	1.8	-	1.8
40	3.9	2.4	1	1	10	2.7	-	2.7	-17	2.0	2.0	2.2	-	2.2	-	2.2	-	2.2
41	4.7	2.7	3	3	7	2.6	-	2.6	-17	2.7	2.7	3.0	-	3.0	-	3.0	-	3.0
42	-	2.5	3	3	14	2.7	-	2.7	9	2.3	2.3	2.9	-	2.9	-	2.9	-	2.9
43	-	2.4	3	3	9	2.7	-	2.7	22	2.7	2.7	3.0	-	3.0	-	3.0	-	3.0
44	4.1	2.7	3	3	8	2.7	-	2.7	-	-	-	-	-	-	-	-	-	-
45	3.7	2.7	3	3	15	2.6	-	2.6	-	-	-	-	-	-	-	-	-	-
46	1.9	2.5	2	2	18	2.5	-	2.5	-	-	-	-	-	-	-	-	-	-
47	4.3	2.7	2	2	18	2.7	-	2.7	-	-	-	-	-	-	-	-	-	-
48	2.4	2.0	1	1	20	2.0	-	2.0	-2	2.1	2.1	2.2	-	2.2	-	2.2	-	2.2
49	-2.1	1.8	1	1	15	1.8	-	1.8	-43	1.2	1.2	1.1	-	1.1	-	1.1	-	1.1
50	1.4	1.8	1	1	12	1.8	-	1.8	-8	2.0	2.0	1.6	-	1.6	-	1.6	-	1.6

TABLE XIII (continued)

Serial No.	X 1	X 2	X 7	Y 1	X 3	X 4	Y 2	X 3	X 6	Y 3	Y 4	Y 5
51	10.1	4.2	3	3.0	1000	5	3.0	1.1	30	2.9	3.0	3.0
52	3.7	3.7	3	2.6	950	16	2.1	-.3	-	-	-	-
53	-1.3	3.7	3	2.2	950	15	2.1	0.0	-	-	-	-
54	-4.0	3.4	1	1.9	940	-	-	-1.4	-18	1.5	1.3	-
55	-3.9	2.1	1	1.6	890	11	1.1	-	-35	1.6	1.2	1.0
56	-4.4	3	3	1.7	920	19	1.4	.2	-1	2.3	1.9	1.6
57	2.4	2.8	2	2.5	950	8	2.3	.3	-	-	-	-
58	-9.7	2.6	3	2.0	960	11	2.5	.5	-	-	-	-
59	-2.7	3.2	3	2.2	980	10	2.7	.5	-26	1.7	1.8	2.0
60	-2.0	3.9	3	2.2	990	12	2.3	.5	5	2.3	2.4	2.5
61	2.2	4.0	2	2.5	970	13	2.4	-.9	-22	1.8	1.7	1.8
62	2.6	3.8	3	2.5	960	18	2.5	.1	12	2.4	2.8	2.9
63	5.4	4.2	3	2.7	970	14	2.4	.3	-	-	-	-
64	1.6	3.9	3	2.5	960	16	2.4	.4	-	-	-	-
65	2.7	3.5	3	2.4	960	15	2.4	.2	18	3	2.9	2.8
66	-.7	2.2	3	1.9	960	21	1.8	-.1	-26	1.8	1.6	1.6
67	-.8	3.9	3	2.3	980	15	2.6	-.1	19	2.4	2.7	2.9
68	1.0	2.5	4	2.3	1015	8	3.0	-.9	-	-	-	-
69	-3.8	2.4	3	1.1	910	4	1.8	.3	-54	1.5	1.1	1.1
70	-5.8	4.5	3	2.6	1015	0	3.0	1.0	-40	2.9	3.0	3.0
71	3.5	3.0	3	2.5	1015	10	3.0	.7	28	2.8	2.9	2.9
72	1.6	5.1	3	2.6	960	16	2.4	.2	-9	2.2	2.8	2.8
73	2.7	5.9	3	2.7	950	12	2.2	.1	-6	2.2	2.8	2.8
74	2.1	4.5	3	2.6	950	-	-	.7	-12	1.8	2.0	-
75	-1.4	3.2	2	2.1	920	17	1.2	-.7	-29	-	-	-
76	-1.5	3.3	1	2.1	920	9	1.4	-.4	1	2.1	2.1	1.7

TABLE XIII (continued)

Serial No.	X	X 1	X 2	X 7	Y 1	X 3	Y 2	X 5	X 6	Y 7	Y 4	Y 5
77	1.3	1.6	2	2	2.1	970	2.5	-	-	-	-	-
78	3.2	1.7	1	1	2.4	960	2.4	-	-	-	-	-
79	-2.2	2.0	1	1	1.1	900	1.1	-	-	-	-	-
80	-2.3	1.2	1	1	1.2	920	1.2	-	-	-	-	-
81	-2.0	.5	1	1	1.1	910	1.1	0.0	12	2.4	1.9	1.2
82	-2.6	.2	1	1	1.9	940	1.9	.8	15	1.8	1.2	1.2
83	3.3	3.4	3	3	2.9	1000	2.9	.5	54	2.7	2.9	3.0
84	6.4	3.4	3	3	3.0	1000	3.0	0.0	18	2.4	2.9	3.0
85	10.9	3.9	3	3	2.8	990	2.8	.8	1	2.5	2.9	3.0
86	12.5	4.9	3	3	3.0	1015	3.0	.6	5	2.6	3.0	3.0
87	8.4	5.3	3	3	-	990	-	0.0	10	2.1	2.8	-
88	.1	4.3	1	1	1.4	930	1.4	.5	-	-	-	-
89	-1.4	.3	1	1	1.8	950	1.8	.1	-	-	-	-
90	-1.7	.7	2	2	-	940	-	.5	11	2.2	1.5	-
91	-5.5	-1.3	2	2	-	980	-	.4	14	2.2	1.3	-
92	5.2	.6	3	3	-	1000	-	1.1	24	2.9	3.0	-
93	10.2	4.2	3	3	-	1000	-	1.9	22	3.0	3.0	-
94	8.6	7.8	3	3	3.0	1015	3.0	1.4	49	3.0	3.0	3.0
95	10.0	6.3	3	3	3.0	1015	3.0	.3	13	2.5	2.9	3.0
96	5.9	7.9	3	3	3.0	1015	3.0	.7	-	-	-	-
97	-1.4	4.9	3	3	2.4	960	2.4	.9	-	-	-	-
98	5.2	2.5	3	3	2.6	990	2.6	.9	-	-	-	-
99	6.6	2.2	3	3	2.7	980	2.7	.2	3	2.7	2.8	2.9
100	5.2	2.9	2	2	2.8	990	2.8	.4	8	2.5	2.9	3.0
101	2.5	-1.5	2	2	2.5	980	2.5	.5	32	2.2	1.8	1.9
102	1.9	-1.9	1	1	2.4	960	2.4	-1.4	43	1.2	1.1	1.2

TABLE XIII (continued)

Serial No.	X ₁	X ₂	X ₇	X ₁	X ₃	X ₄	Y ₂	X ₅	X ₆	Y ₃	Y ₄	Y ₅
103	-1.4	-1.1	1	1.4	940	14	1.8	.1	-21	1.9	1.3	1.3
104	-2.8	-2.9	1	1.1	850	-	-	.9	4	1.9	1.1	-
105	7.3	2.2	3	2.8	980	0	2.9	1.8	27	3.0	3.0	3.0
106	9.5	7.6	3	3.0	1015	6	3.0	1.6	49	3.0	3.0	3.0
107	3.9	3.0	3	2.6	980	14	2.6	.1	2	2.3	2.8	2.9
108	2.1	3.9	3	2.5	980	8	2.7	.5	11	2.6	2.9	3.0
109	2.3	3.1	3	2.5	1000	12	2.9	.4	13	2.6	2.9	3.0
110	5.9	3.8	2	2.6	950	17	2.0	-.7	-50	1.4	1.5	1.6
111	8.1	1.8	2	2.8	960	10	2.4	.6	15	2.7	3.0	2.9
112	-.6	4.5	1	1.7	950	18	2.0	-.7	-17	1.9	1.6	1.7
113	-1.0	3.8	1	1.1	910	0	2.2	1.1	-49	2.1	1.2	1.3
114	3.6	2.5	3	2.6	990	6	2.8	1.6	29	3.0	3.0	3.0
115	5.7	2.9	3	2.7	930	11	2.8	.4	14	2.5	2.9	3.0
116	-.2	1.0	3	1.7	950	16	2.1	.3	14	2.6	2.8	2.8
117	-1.0	1.5	1	1.4	930	24	1.1	1.0	-20	1.6	1.2	1.0
118	-1.9	-.5	1	1.5	920	18	1.2	.3	-35	1.5	1.1	1.0
119	-.6	1.5	1	1.4	920	18	1.2	.3	-	-	-	-
120	-1.4	2.2	1	1.3	920	18	1.2	.1	-	-	-	-
121	-.1	2.2	1	1.3	900	11	1.1	1.1	-	1.9	1.2	1.0
122	1.6	2.5	1	1.9	950	17	2.0	.1	6	2.4	2.2	2.1
123	-2.3	2.6	1	1.1	900	-	-	.1	7	2.4	2.2	-
124	1.1	2.2	1	1.7	950	-	-	.1	-26	1.8	1.1	-
125	-1.0	2.8	1	1.4	910	13	1.1	.3	39	2.4	2.0	1.1
126	1.3	1.2	3	2.0	970	12	2.6	.1	4	2.1	1.8	2.3
127	1.9	2.0	2	2.1	970	14	2.5	.1	5	2.3	2.2	-
128	1.9	1.8	3	2.2	960	16	2.4	.4	-	-	-	-

TABLE XIII (continued)

Serial No.	X ₁	X ₂	X ₇	Y ₁	X ₃	X ₄	Y ₂	X ₅	X ₆	Y ₃	Y ₄	Y ₅
129	3	1.9	3	2.0	960	16	2.4	.4	-	2.2	2.8	-
130	6.2	2.7	3	2.7	950	14	2.4	-.2	6	2.3	2.9	2.9
131	10.8	2.3	3	3.0	950	16	2.1	.3	0	2.6	2.9	2.9
132	7.6	3.1	3	2.8	970	12	2.6	.4	15	2.6	2.9	3.0
133	5.7	3.9	3	2.7	1000	10	2.9	.6	12	2.6	2.9	3.0
134	4.2	3.6	3	2.6	1000	17	2.7	.1	10	2.4	2.8	2.9
135	2.5	3.3	2	2.5	970	20	2.2	-1.0	-23	1.6	1.7	1.8
136	6.9	2.8	3	2.8	990	12	2.8	.6	-11	2.2	2.8	2.9
137	6.5	4.7	3	2.8	1000	8	2.9	.5	16	2.6	2.9	3.0
138	3.2	4.4	3	2.6	960	19	2.2	0.0	-19	1.9	2.2	2.2
139	2.5	4.0	3	2.5	950	15	2.2	-.2	10	2.3	2.8	2.8
140	2.0	2.5	3	2.4	930	20	1.3	0.0	-	2.2	2.5	1.9
141	3.5	-.3	3	-	990	13	-	-.2	3	-	-	-
142	3.4	-.8	3	1.9	1015	2	3.0	.2	6	2.0	1.9	2.0
143	4.3	3.8	3	2.6	1000	10	2.9	.2	-18	2.6	2.9	3.0
144	3.1	3.9	2	2.6	990	15	2.7	-.1	29	2.2	2.8	2.9
145	1.8	5.0	3	2.6	1000	18	2.7	-.1	1	2.3	2.8	2.9
146	3.5	5.0	3	2.7	980	13	2.7	.4	22	2.6	2.9	3.0
147	8.4	5.0	3	2.9	970	12	2.6	.1	-20	1.9	2.5	2.7
148	10.2	3.8	3	3.0	990	8	2.8	.3	23	2.6	3.0	3.0
149	5.0	5.0	3	2.7	1000	15	2.8	.3	-10	2.2	2.8	2.9
150	7.7	4.4	3	2.9	990	8	2.8	.7	-	-	-	-
151	8.5	5.0	3	2.9	1000	10	2.9	.2	-	-	-	-
152	7.7	4.8	3	2.9	980	10	2.7	.4	-16	2.1	2.8	2.9
153	8.7	2.5	1	2.9	950	20	1.8	-.5	-19	1.8	2.0	1.8
154	6.6	4.7	3	2.5	950	10	2.2	0.0	2	2.3	2.8	2.8
155	1.4	2.3	2	2.3	950	15	2.2	-.4	-	2.0	2.2	2.2

TABLE XIII (continued)

Serial No.	X ₁	X ₂	X ₇	Y ₁	X ₃	X ₄	Y ₂	X ₅	X ₆	Y ₃	Y ₄	Y ₅
156	5.3	3.3	3	2.7	960	11	2.5	.6	0	2.4	2.9	2.9
157	4.3	4.3	3	2.7	1000	8	2.9	.3	21	2.6	2.9	3.0
158	4.6	3.4	3	2.6	1015	16	2.9	.4	7	2.5	2.9	3.0
159	6.1	5.2	3	2.8	1015	14	3.0	.2	47	2.6	2.9	3.0
160	3.5	4.4	2	2.6	990	18	2.6	.4	-43	1.5	1.6	1.8
161	3.4	4.1	1	2.6	960	18	2.3	0.0	-21	1.9	2.2	2.2
162	4.9	3.1	3	2.6	940	18	1.7	-.6	-16	1.8	2.0	1.8
163	1.6	4.3	3	2.5	940	-	-	-.2	9	2.2	2.7	-
164	2.1	1.9	3	2.3	940	18	1.7	-.2	0	2.2	2.4	2.1
165	1.4	3.2	3	2.4	950	18	2.0	-.3	3	2.2	2.5	2.4
166	-1.3	1.2	2	1.7	960	14	2.6	-.4	1	2.1	1.7	1.3
167	-1.0	-1.5	1	1.3	970	10	2.6	-1.1	-23	1.5	1.1	1.2
168	-.7	-5.4	1	1.0	940	8	2.0	-.1	-20	1.9	1.1	1.2
169	-.3	4.2	3	2.4	990	0	2.9	-.2	45	2.3	2.7	2.9
170	3.7	2.3	2	2.5	1000	14	2.9	-.4	2	2.1	2.5	2.7
171	-.9	-3.1	1	1.1	950	20	1.7	-1.3	-62	1.1	1.1	1.1
172	-1.4	-1.5	1	1.3	900	11	1.1	-.6	-17	1.8	1.2	1.0
173	4.3	2.3	3	2.6	950	3	2.5	.6	-	-	-	-
174	7.0	4.8	3	2.9	960	10	2.9	.4	-	2.5	2.9	3.0
175	7.9	6.7	3	3.0	1000	7	2.9	.3	15	2.5	2.9	3.0
176	4.4	6.6	3	2.8	990	12	2.8	.1	20	2.4	2.9	3.0
177	1.4	6.2	3	2.7	1000	13	2.9	0.0	10	2.5	2.9	3.0
178	0.0	4.9	2	2.5	980	13	2.6	.2	14	2.5	2.9	2.9
179	.5	3.2	1	2.3	940	22	1.4	-1.0	-64	1.2	1.2	1.0
180	-.6	1.5	1	1.8	920	18	1.2	-.6	-16	1.8	1.8	1.1
181	-.9	-.6	1	1.3	890	3	1.5	-.1	6	2.1	1.4	1.2
182	1.7	2.5	3	2.4	980	5	2.7	1.1	21	2.9	2.9	3.0

TABLE XIV

MARINE PENETRATION FORECAST CHECK DATA

Serial No.	X ₁	X ₂	X ₇	Y ₁	X ₃	X ₄	Y ₂	X ₅	X ₆	Y ₃	Y ₄	Y ₅
1	-3.1	-	1	1.3	940	16	1.7	-1.0	-	-	-	-
2	1.0	.3	2	1.8	970	16	2.5	-.3	-12	1.9	1.6	1.7
3	4.7	1.0	1	2.3	940	18	1.6	-.5	5	1.9	2.1	2.2
4	-1.1	-3.1	1	1.1	910	15	1.1	-.4	-39	1.5	1.0	1.0
5	2.3	2.2	3	2.3	970	10	2.6	-.1	57	2.4	2.7	2.8
6	2.8	2.4	3	2.4	980	17	2.6	-.1	45	2.4	2.8	2.9
7	-1.4	.9	2	1.5	950	18	2.0	-.6	3	2.0	1.5	1.7
8	-2.7	.3	1	1.4	970	18	2.4	-.4	-26	1.4	1.1	1.2
9	6.1	.6	3	2.5	960	16	2.4	.4	3	2.3	2.8	2.9
10	5.1	3.5	3	2.6	1015	5	3.0	.5	40	2.7	2.9	3.0
11	5.5	4.1	3	2.7	1015	5	3.0	.6	44	2.7	2.9	3.0
12	3.2	4.9	3	2.6	1000	16	2.8	-.3	-	2.0	2.4	2.5
13	2.8	6.9	2	2.7	950	14	2.6	-.1	-9	2.1	2.3	2.5
14	-5.4	.3	1	1.3	930	20	1.3	-1.9	-66	1.0	1.0	1.0
15	-4.7	-1.3	1	1.1	pcue	12	1.0	-2.1	-20	1.3	1.0	1.0
16	4.1	2.3	3	2.5	970	12	2.6	0.0	45	2.0	2.3	2.4
17	-	2.4	3	-	1015	5	3.0	-.1	34	2.0	-	-
18	1.9	1.1	2	2.0	960	15	2.1	-1.6	-24	1.4	1.2	1.3
19	5.1	2.4	3	2.6	960	15	2.4	0.0	-12	2.0	2.4	2.4
20	-1.0	1.5	3	1.7	950	20	1.8	-.5	-6	2.0	1.6	1.7
21	-.7	2.6	2	1.9	980	10	2.7	-.2	-16	2.3	2.1	2.2
22	2.7	2.1	3	2.4	960	17	2.4	-.4	-11	1.9	2.1	2.2
23	9.1	4.5	3	2.9	1015	4	3.0	.7	20	2.8	3.0	3.0
24	8.8	6.9	3	3.0	990	10	2.8	-.2	41	2.3	2.9	3.0

TABLE XIV (continued)

Serial No.	X ₁	X ₂	X ₇	Y ₁	X ₃	X ₄	Y ₂	X ₅	X ₆	Y ₃	Y ₄	Y ₅
25	4.1	4.4	2	2.6	990	18	2.6	-.6	-14	1.8	2	2.1
26	3.7	4.0	2	2.5	969	15	2.4	-.7	-5	1.9	2	2.1
27	.3	2.9	2	2.1	970	16	2.5	-.1	-14	2.0	2	2.1
28	.3	1.9	3	1.6	980	8	2.7	-.9	-1	1.9	1.7	1.8
29	-.7	4.6	2	2.4	990	12	2.8	-.5	-4	2.0	2.2	2.2
30	-1.0	.6	1	1.6	940	20	1.5	-2.5	-33	1.0	1.0	1.0
31	-0.0	1.0	1	1.7	970	15	2.5	-.1	3	2.2	1.8	1.9
32	-5.8	-3.7	1	1.0	none	10	1.1	-1.1	-37	1.3	1.0	1.0
33	-1.0	2.0	2	1.7	960	15	2.4	-.5	28	2.2	1.8	1.9
34	-2.3	1.3	3	1.6	950	18	2.0	-.1	6	2.3	1.8	1.8
35	1.7	3.7	3	2.4	970	12	2.6	-.4	25	2.6	2.8	2.9
36	3.5	5.2	3	2.9	1015	8	3.0	.3	20	2.5	2.9	3.0
37	2.7	5.1	3	2.6	980	14	2.6	0.0	7	2.4	2.8	2.9
38	5.1	4.5	2	2.7	990	16	2.7	-.9	-17	1.7	1.8	2.1
39	3.7	4.6	2	2.6	1000	20	2.6	-.5	-11	1.9	2.0	2.1
40	3.8	4.8	3	2.6	970	14	2.5	-.8	18	2.8	2.9	2.9
41	4.1	4.1	2	2.6	970	22	1.9	-.5	-5	2.0	2.3	2.2
42	4.4	4.1	1	1.6	930	20	1.3	-.8	-35	1.4	1.1	1.0
43	3.3	2.2	3	2.4	950	15	2.2	-.1	10	2.3	2.3	2.9
44	5.5	2.8	3	2.6	970	16	2.5	-.6	9	2.1	2.5	2.6
45	5.1	3.0	1	2.6	930	19	1.4	-.4	-10	1.9	2.2	1.7
46	1.4	.7	1	1.6	920	16	1.2	-.3	-24	1.6	1.2	1.1
47	4.1	2.9	3	2.5	960	9	2.5	-.2	40	2.5	2.9	2.9
48	2.7	3.2	2	2.5	970	16	2.5	-.4	-4	2.0	2.4	2.4
49	1.7	2.1	3	2.2	960	20	2.4	-.5	-4	2.0	2.1	2.2
50	11.1	4.7	3	3.0	1015	5	3.0	-.8	11	2.7	3.0	3.0

TABLE XIV (continued)

Serial No.	X ₁	X ₂	X ₇	Y ₁	X ₃	X ₄	Y ₂	X ₅	X ₆	Y ₃	Y ₄	Y ₅
51	12.5	8.6	3	3.0	1015	6	3.0	1.5	33	3.0	3.0	3.0
52	6.7	8.9	2	3.0	1000	20	2.5	0.0	-27	1.8	2.0	2.1
53	.7	3.4	3	2.5	1000	20	2.5	-.2	-4	2.1	2.4	2.4
54	.7	3.3	3	2.1	960	16	2.4	-.7	6	2.0	2.0	2.1
55	.4	4.1	3	2.4	960	20	2.0	0.0	6	2.3	2.7	2.6
56	-4.1	4.2	3	2.0	970	20	2.2	-.2	-8	2.0	1.9	1.9
57	0.0	.2	2	1.6	940	22	1.4	-.2	-22	1.8	1.4	1.1
58	5.1	4.2	3	2.7	960	13	2.5	-.1	-9	2.0	2.3	2.4
59	1.3	-1.7	1	1.4	1000	15	2.3	-.6	9	1.9	1.3	1.4
60	10.1	8.1	3	3.0	1015	5	3.0	2.7	0	3.0	3.0	3.0
61	6.1	4.2	1	2.7	990	14	2.8	-.8	7	2.0	2.4	2.5
62	1.7	-8.4	1	1.0	920	20	1.2	-1.4	-34	1.1	1.0	1.0

TABLE IV

MAXIMUM TEMPERATURE FORECAST DATA
(ACTUAL VALUES OF $x_1, x_2, x_3, x_4, x_5, x_6, x_7, x_8$ AND
COMPUTED VALUES OF z_1, z_2, z_3, z_4, z_5)

Serial No.	x_1	x_2	x_7	z_1	x_3	x_5	z_2	x_6	x_8	z_3	z_4	z_5
1	5.0	-1.4	76	84	910	-1.3	78	8	72	80	79	77
2	3.7	.5	83	87	940	-.6	86	10	74	80	85	80
3	3.1	.4	80	87	940	-.5	87	14	88	88	85	85
4	2.4	-.2	76	86	920	-.8	82	14	89	89	82	83
5	.7	-.1	75	85	920	-.9	82	15	95	92	82	84
6	-2.0	-1.5	72	81	920	-.4	83	10	84	87	81	82
7	-2.7	-1.2	72	80	910	0.0	82	12	77	82	80	79
8	-1.7	-3.0	70	78	none	-.3	77	10	72	78	76	73
9	2.7	-2.2	82	82	930	-.5	84	8	79	84	82	81
10	.8	1.7	94	89	950	-.6	89	10	93	93	89	90
11	0.0	1.3	92	88	960	-.6	91	17	94	92	90	90
12	2.4	-3.0	85	80	960	-.5	91	10	81	85	85	83
13	1.7	-.2	85	86	none	-.3	77	8	79	84	80	80
14	-4.0	-3.3	76	76	none	-1.1	75	11	72	78	74	73
15	3.1	-1.0	81	84	none	.8	79	5	68	78	80	76
16	9.1	1.5	86	90	960	1.2	94	5	78	86	96	92
17	-1.7	-.3	75	83	930	-1.4	81	12	78	82	81	79
18	2.1	2.3	90	92	950	.8	92	6	79	86	93	90
19	6.2	4.0	96	98	1000	0.0	95	10	85	88	98	95
20	6.9	4.9	90	98	960	.3	93	17	92	91	96	95
21	5.2	1.8	81	92	950	-.7	93	14	97	96	94	95
22	3.4	.6	79	83	930	-.4	85	-	93	-	85	-

TABLE XV (continued)

Serial No.	X ₁	X ₂	X ₇	Z ₁	X ₃	X ₅	Z ₂	X ₄	X ₈	Z ₃	Z ₄	Z ₅
23	.3	2.0	79	90	910	0.0	83	16	93	91	84	85
24	.4	.1	76	86	920	-.3	83	15	80	83	83	81
25	2.9	-2.8	73	81	940	-.5	87	14	79	83	83	81
26	4.6	-4.3	61	79	940	-.1	90	3	69	80	84	80
27	8.1	1.7	90	94	980	.5	95	7	79	85	96	91
28	8.2	4.7	97	99	990	.5	98	4	82	90	99	97
29	5.6	6.0	95	99	1000	.2	97	8	90	93	99	99
30	-2.6	1.4	72	84	930	-1.4	81	19	84	84	81	80
31	5.5	5.5	96	98	930	0.0	95	8	98	94	97	98
32	-	2.9	93	91	960	-.5	91	16	94	92	92	92
33	5.0	4.2	102	97	960	.4	93	13	93	92	96	96
34	5.2	6.2	99	99	970	0.0	94	4	99	100	97	101
35	-	3.4	85	91	940	-.5	87	18	99	94	89	90
36	1.4	2.6	92	92	950	-.2	91	12	97	94	93	94
37	6.7	3.3	92	96	950	-.1	91	16	96	93	94	94
38	3.9	3.4	87	95	970	-.2	93	15	96	93	35	95
39	1.3	.5	87	87	970	.5	94	14	88	89	92	90
40	3.9	.9	86	89	960	.2	95	10	83	86	94	90
41	4.7	5.1	95	97	970	.6	95	7	85	90	97	95
42	.1	3.1	93	92	960	-.1	92	14	90	90	93	92
43	.6	3.6	100	93	980	.6	97	9	93	94	96	97
44	4.1	4.5	101	96	980	.3	96	8	99	98	97	100
45	3.7	4.8	97	97	980	.3	94	15	101	96	96	95
46	1.9	6.5	95	96	980	-.4	94	18	99	94	96	97
47	4.3	3.9	92	96	1000	0.0	98	16	93	91	98	97
48	2.4	2.9	86	93	960	-.4	91	20	97	93	93	93

TABLE IV (continued)

Serial No.	X ₁	X ₂	X ₇	Z ₁	X ₃	X ₅	Z ₂	X ₄	X ₈	Z ₃	Z ₄	Z ₅
49	-2.1	-.9	85	82	940	-1.4	82	15	85	86	81	82
50	1.4	-1.1	89	83	940	-.3	82	12	85	87	84	84
51	10.1	4.2	97	99	1000	1.1	101	5	88	93	100	100
52	3.7	3.7	93	95	950	-.3	91	16	90	89	94	92
53	-1.3	3.7	93	90	950	0.0	91	15	93	92	91	91
54	-4.0	3.4	82	83	940	-1.4	82	-	94	-	81	-
55	-3.9	2.1	83	83	890	-.3	73	11	86	88	79	81
56	-.4	-.3	88	86	820	-.2	85	10	84	87	84	84
57	2.4	2.8	92	93	950	-.2	91	8	88	92	93	93
58	-.9	2.6	96	89	960	-.5	93	11	93	93	92	92
59	-.7	3.2	96	88	980	-.5	93	10	96	95	93	95
60	-2.0	3.9	100	88	990	-.1	96	12	95	94	93	94
61	1.2	4.0	92	93	970	-.9	91	18	95	92	93	93
62	2.6	3.8	92	94	960	-.1	93	12	94	92	95	95
63	3.4	4.2	98	97	970	-.3	93	12	94	94	96	97
64	1.6	3.9	96	94	960	-.4	91	16	97	93	94	95
65	-.2	3.5	92	92	960	-.2	92	15	98	94	93	94
66	-.7	2.2	93	89	960	-.1	92	21	92	90	91	90
67	-.6	3.9	93	91	980	-.1	95	15	94	92	94	94
68	-1.0	2.5	93	92	1015	-.9	97	8	95	95	86	97
69	-3.8	-2.4	86	77	910	-.3	82	4	80	83	78	80
70	5.8	4.5	92	97	1015	1.0	101	0	87	96	100	102
71	3.5	3.0	96	94	1015	-.7	101	10	87	94	98	100
72	1.6	5.1	90	95	960	-.2	93	16	95	91	95	94
73	2.7	5.9	98	97	950	-.1	91	12	97	94	95	96
74	2.1	4.5	93	95	950	-.7	88	-	96	-	92	-
75	-1.4	3.2	90	89	920	-.7	88	17	67	87	-	-

TABLE IV (continued)

Serial No.	X ₁	X ₂	X ₇	Z ₁	X ₃	X ₅	Z ₂	X ₄	X ₈	Z ₃	Z ₄	Z ₅
76	-1.5	3.3	86	89	920	-	83	9	89	91	84	85
77	1.3	1.6	89	90	970	-	93	24	87	86	93	90
78	3.2	1.7	96	91	960	-	92	15	83	83	92	90
79	2.2	2.0	86	89	900	-	81	12	81	84	83	82
80	-2.3	1.2	84	86	920	-	83	16	83	84	82	81
81	-2.8	5	86	85	910	-	82	13	87	80	82	83
82	-2.6	2.2	89	82	940	-	95	10	79	84	82	81
83	3.3	3.4	90	94	1000	-	100	7	90	93	98	99
84	6.4	3.4	97	96	1000	-	100	3	91	96	98	100
85	10.9	3.9	97	93	990	-	99	4	96	93	98	104
86	12.5	4.9	98	102	1015	-	101	5	92	93	100	104
87	8.4	5.3	94	100	990	-	97	-	93	95	102	-
88	1.4	4.3	84	72	730	-	84	13	93	-	99	86
89	-1.4	3.3	82	84	950	-	91	20	93	90	87	87
90	-5.5	7.7	90	93	940	-	57	-	82	-	84	-
91	-5.2	-1.3	84	76	960	-	94	-	90	-	84	-
92	5.2	4.6	90	83	1000	-	101	-	83	-	96	-
93	10.2	4.2	95	89	1000	-	101	-	95	-	100	-
94	8.6	7.8	104	102	1015	-	101	0	100	-	102	106
95	10.0	6.3	107	102	1015	-	100	4	104	-	102	106
96	5.9	7.9	103	101	1015	-	100	8	105	-	101	105
97	-1.4	4.9	93	91	960	-	91	20	103	-	91	93
98	5.2	2.5	92	93	990	-	94	17	99	-	95	95
99	6.6	2.2	98	93	980	-	95	10	97	-	95	96
100	5.2	2.9	100	94	990	-	95	5	95	-	97	100
101	2.5	-1.5	89	83	950	-	93	13	86	-	88	86
102	1.9	-1.9	79	82	960	-	86	14	83	-	83	82

TABLE IV (continued)

Serial No.	r_1	x_2	x_7	z_1	x_3	x_5	z_2	x_8	x_9	z_3	z_4	z_5
103	-1.4	-1.1	85	82	940	.1	90	14	80	83	85	93
104	-2.8	-2.3	82	77	950	-.9	77	-	74	-	75	-
105	7.3	2.2	89	94	930	1.2	99	0	90	91	97	95
106	9.5	7.6	99	102	1016	1.6	101	6	92	95	102	104
107	9.7	3.0	99	94	930	.1	95	14	95	93	96	96
108	2.1	3.3	102	94	980	.5	96	3	97	97	96	93
109	2.3	3.1	97	93	1000	.4	100	12	99	95	98	100
110	5.3	.3	89	89	960	-.7	89	17	91	90	89	89
111	6.1	1.8	93	84	960	-.6	93	10	94	94	95	95
112	-.6	.6	38	86	990	-.7	89	1	92	90	86	86
113	-1.0	-4.5	34	76	910	1.1	84	0	81	92	73	82
114	3.6	3.8	91	95	990	1.6	100	6	85	90	98	96
115	5.7	2.5	95	93	990	-.4	94	11	89	91	97	90
116	-.2	2.9	96	91	960	.5	92	16	94	92	92	92
117	-1.0	1.0	36	86	930	-1.0	83	24	92	89	93	84
118	-1.9	-.5	30	82	920	-.5	83	13	84	84	81	80
119	-.6	-.1	84	84	920	-.3	84	16	81	83	83	81
120	-1.8	-.5	80	83	920	-2.1	77	18	76	79	79	75
121	-.1	-2.2	84	81	900	-1.1	70	11	75	81	76	76
122	1.6	.5	76	87	950	.1	91	17	79	82	90	85
123	-2.3	-2.6	78	79	920	.1	91	-	72	-	76	-
124	1.1	-.2	84	85	950	-.1	91	-	80	-	88	-
125	-1.0	-.8	85	83	910	-.5	81	13	84	86	81	81
126	1.3	1.2	91	88	970	-.1	93	12	86	88	91	89
127	.9	2.0	90	90	970	-.1	93	16	88	89	93	91
128	1.9	1.6	94	91	960	.4	93	16	88	88	93	91

TABLE XV (continued)

Serial No.	X ₁	X ₂	X ₇	Z ₁	X ₃	X ₅	Z ₂	X ₄	X ₂	Z ₃	Z ₄	Z ₅
129	3	1.9	98	90	960	.4	93	16	94	92	93	93
130	6.2	2.7	95	94	960	-.2	92	14	93	92	94	94
131	10.8	2.3	93	97	950	.3	91	16	94	92	95	95
132	7.6	3.1	101	96	970	.4	94	12	97	94	96	97
133	5.7	3.9	104	97	1000	.6	100	10	100	97	99	102
134	4.2	3.6	100	95	1000	.1	99	17	101	95	98	100
135	2.5	3.3	95	93	970	-1.0	90	20	99	94	92	93
136	6.9	2.8	98	95	990	.6	99	12	94	93	95	96
137	6.5	4.7	98	98	1000	.5	100	8	97	96	100	102
138	3.2	4.4	94	96	960	0.0	92	19	97	93	95	95
139	2.5	4.0	96	95	950	-.2	91	15	97	93	94	97
140	2.0	2.5	90	92	930	0.0	86	20	104	96	89	91
141	3.5	5	68	85	990	-.2	96	13	97	94	92	93
142	3.4	5.8	98	84	1015	.2	100	2	90	96	93	95
143	4.3	3.8	102	96	1000	.2	99	10	98	96	98	100
144	3.1	3.9	102	95	990	-.1	96	15	99	94	97	98
145	1.8	5.0	100	95	1000	-.1	95	18	104	97	97	100
146	3.5	5.0	106	97	980	.4	96	13	104	99	97	101
147	8.4	5.0	104	100	970	.1	94	12	101	97	97	100
148	10.2	3.8	107	92	990	.3	97	8	105	103	95	103
149	5.0	5.0	105	98	1000	.3	100	15	104	98	100	104
150	7.7	4.4	104	98	990	.7	99	8	107	104	99	105
151	8.5	5.0	102	100	1000	.2	100	10	103	100	101	105
152	7.7	4.8	99	99	980	.4	96	10	102	99	93	102
153	8.7	2.5	87	96	950	-.5	90	20	99	94	94	95
154	6.6	4.7	96	93	950	0.0	91	10	100	97	95	97
155	1.4	2.3	92	91	950	-.4	90	15	101	96	91	93

TABLE XV (continued)

Serial No.	X ₁	X ₂	X ₇	Z ₁	X ₃	X ₅	Z ₂	X ₄	X ₈	Z ₃	Z ₄	Z ₅
156	5.3	3.3	93	95	960	.6	94	11	100	97	95	98
157	4.3	4.3	105	97	1000	.3	100	3	100	99	99	103
158	4.6	3.8	104	95	1015	.4	100	16	100	95	90	100
159	6.1	5.2	106	99	1015	.2	100	16	104	99	100	104
160	3.5	4.8	99	96	990	.4	95	13	101	95	96	95
161	3.8	4.1	90	96	980	0.0	92	16	93	93	95	95
162	4.9	3.1	91	94	940	.6	86	13	93	93	90	91
163	1.6	4.3	90	94	940	.2	90	-	95	-	93	-
164	2.1	1.9	90	91	960	.2	89	18	93	91	90	90
165	1.6	3.2	94	93	950	.3	91	18	93	91	93	92
166	-1.3	1.2	94	86	960	.4	91	16	93	92	99	87
167	-1.0	-1.5	83	82	970	-1.1	90	13	88	93	85	86
168	-	-5.8	85	75	940	.1	90	6	83	77	81	82
169	3.7	4.2	95	93	990	.2	96	0	90	93	96	100
170	-	2.3	92	92	1000	.4	97	18	89	89	96	94
171	-	-3.1	78	79	950	-1.3	85	20	82	83	80	79
172	-1.8	-1.5	76	81	900	.6	79	11	76	81	73	76
173	4.3	2.3	90	93	950	.6	92	3	75	85	75	90
174	7.0	4.3	95	93	950	.4	92	10	91	92	96	95
175	7.3	6.7	93	101	1000	.3	100	7	91	94	101	102
176	8.4	6.3	100	99	990	.1	97	12	90	95	93	100
177	1.6	6.2	104	96	1000	0.0	96	13	100	96	93	100
178	0.0	4.9	98	93	950	.2	96	13	100	96	96	98
179	5	3.2	81	92	960	-1.0	84	22	97	92	87	85
180	-	1.5	78	83	920	.6	82	16	91	80	81	83
181	-	-1.6	94	81	890	.1	79	3	79	83	76	80
182	1.7	-2.5	90	92	960	1.1	97	5	86	83	96	96

TABLE XVI

MAXIMUM TEMPERATURE FORECAST CHECK DATA

Serial No.	X ₁	X ₂	X ₇	Z ₁	X ₃	X ₅	Z ₂	X ₄	X ₈	Z ₃	Z ₄	Z ₅
1	3.1	5.3	100	97	990	1.0	100	12	100	97	99	101
2	0.0	3.5	91	91	950	-.3	91	12	96	94	91	92
3	2.7	3.6	95	94	950	.7	92	17	94	92	94	94
4	8.3	5.1	99	100	970	1.7	96	9	97	95	93	100
5	5.4	5.4	102	95	990	1.0	100	10	100	97	99	101
6	4.4	5.3	99	97	1000	1.0	101	11	102	99	100	103
7	1.6	4.1	86	94	970	1.1	95	14	101	95	96	97
8	-.7	2.2	93	89	950	0.0	91	16	102	96	90	92
9	2.4	4.9	95	96	950	.7	92	15	95	93	95	94
10	0.0	3.6	96	92	970	.7	95	14	98	96	95	95
11	-1.1	3.4	96	90	960	.3	93	13	94	91	93	93
12	6.1	4.7	101	98	1010	1.3	102	4	99	101	101	104
13	5.7	4.4	99	97	1015	1.0	102	10	104	101	100	103
14	6.4	5.2	102	99	1015	1.0	102	8	102	100	101	104
15	7.3	5.3	99	99	1000	.7	100	1	103	100	9	103
16	2.7	2.8	97	97	990	0.0	97	9	95	96	98	100
17	3.4	4.9	95	96	1000	.3	100	2	90	96	95	100
18	2.0	5.3	94	95	960	.7	94	11	95	95	95	95
19	5.7	6.3	94	100	950	.7	92	13	97	93	97	96
20	3.0	5.4	99	99	970	1.1	95	14	93	92	97	96
21	.3	4.8	93	93	970	1.0	95	10	99	97	95	97
22	3.4	5.2	97	96	970	.4	94	12	99	94	96	96
23	4.1	5.3	83	93	960	0.0	92	12	99	94	96	96
24	-1.4	3.5	91	89	950	1.0	92	13	98	94	91	92

TABLE XVI (continued)

Serial No.	X ₁	X ₂	X ₇	Z ₁	X ₃	X ₅	Z ₂	X ₈	Z ₃	Z ₄	Z ₅
25	-2.7	3.9	95	97	950	1.0	92	97	93	90	91
26	5.1	4.7	99	97	969	1.0	94	95	93	96	93
27	2.0	5.1	92	96	930	1.0	97	100	95	97	96
28	3.0	3.3	83	94	940	.7	91	96	92	94	92
29	-1.4	3.4	93	91	1500	.6	100	95	93	97	96
30	8.4	5.4	93	100	910	1.1	93	102	100	97	96
31	7.1	7.0	101	101	1000	.3	100	102	100	101	101
32	5.1	5.5	97	99	950	.7	97	102	100	101	103
33	9.8	3.2	92	97	930	1.4	93	100	95	93	100
34	2.0	2.6	83	92	960	1.4	93	96	94	96	95
35	4.8	3.6	92	95	950	1.4	93	92	94	94	94
36	6.8	6.9	97	101	1015	.7	101	95	93	93	94
37	6.8	8.6	104	102	1015	1.7	102	101	103	102	101
38	-2.4	4.1	96	87	1000	.3	100	94	91	102	105
39	-3.1	3.5	83	85	1015	.3	99	85	94	95	92
40	-1.7	2.4	37	37	900	0.0	81	86	89	82	94
41	-5.5	.2	86	76	900	.3	80	86	89	82	83
42	-3.3	.2	90	84	none	.4	80	86	89	82	80
43	-3.0	-2.9	70	77	none	.3	77	72	73	79	77
44	-4.7	1.5	61	60	none	1.4	79	72	83	73	73
45	3.7	5.7	83	97	970	2.7	96	82	91	97	95
46	7.5	8.4	92	102	1015	4.4	102	91	92	102	100